LETTER

doi:10.1038/nature25164

Treatment of autosomal dominant hearing loss by *in vivo* delivery of genome editing agents

Xue Gao[1,2,3]†*, Yong Tao[4,5]†*, Veronica Lamas[4], Mingqian Huang[4], Wei-Hsi Yeh[1,2,3,6], Bifeng Pan[7], Yu-Juan Hu[4,5], Johnny H. Hu[1,2,3], David B. Thompson[1,2], Yilai Shu[4,8], Yamin Li[9], Hongyang Wang[4,10], Shiming Yang[10], Qiaobing Xu[9], Daniel B. Polley[4], M. Charles Liberman[4], Wei-Jia Kong[5], Jeffrey R. Holt[7], Zheng-Yi Chen[4]§ & David R. Liu[1,2,3]§

Although genetic factors contribute to almost half of all cases of deafness, treatment options for genetic deafness are limited[1–5]. We developed a genome-editing approach to target a dominantly inherited form of genetic deafness. Here we show that cationic lipid-mediated *in vivo* delivery of Cas9–guide RNA complexes can ameliorate hearing loss in a mouse model of human genetic deafness. We designed and validated, both *in vitro* and in primary fibroblasts, genome editing agents that preferentially disrupt the dominant deafness-associated allele in the *Tmc1* (transmembrane channel-like gene family 1) Beethoven (*Bth*) mouse model, even though the mutant $Tmc1^{Bth}$ allele differs from the wild-type allele at only a single base pair. Injection of Cas9–guide RNA–lipid complexes targeting the $Tmc1^{Bth}$ allele into the cochlea of neonatal $Tmc1^{Bth/+}$ mice substantially reduced progressive hearing loss. We observed higher hair cell survival rates and lower auditory brainstem response thresholds in injected ears than in uninjected ears or ears injected with control complexes that targeted an unrelated gene. Enhanced acoustic startle responses were observed among injected compared to uninjected $Tmc1^{Bth/+}$ mice. These findings suggest that protein–RNA complex delivery of target gene-disrupting agents *in vivo* is a potential strategy for the treatment of some types of autosomal-dominant hearing loss.

Although about 100 deafness-associated alleles have been identified, few treatments are available to slow or reverse genetic deafness[4,5]. Complementation of wild-type alleles, or silencing of dominant-negative mutant alleles, have shown promising results in animal models[6,7]. Nonetheless, current approaches face potential challenges including immunogenicity, oncogenicity, and limitations of viral vectors[8,9].

Cas9-based genome editing agents can mediate targeted gene disruption or repair[10–13]. For applications that seek a one-time, permanent modification of genomic DNA, the delivery of non-replicable, transient Cas9–single guide RNA (sgRNA) ribonucleotide protein (RNP) complexes *in vivo* offers improved DNA specificity and potentially greater safety and applicability[14,15], compared with methods that introduce DNA expressing these agents. Approximately 20% of alleles associated with genetic deafness are dominantly inherited[1]. As Cas9–sgRNA complexes can efficiently disrupt genes through end-joining processes, we sought to design Cas9–sgRNA complexes that selectively disrupt dominant alleles associated with hearing loss.

Many genes linked to genetic hearing loss affect the function of sensory hair cells, which transduce acoustic vibrations into electrical nerve signals. TMC1 is an essential component of mechanotransduction channels in mammalian hair cells[16]. Mutations in *TMC1* have been linked to recessive and dominant genetic deafness in humans[17]. A dominant-negative missense mutation in *TMC1* (p.M418K, c.T1253A) causes reduced single-channel current levels and calcium permeability[16] in hair cells, and progressive post-lingual sensorineural hearing loss in humans[18–20]. The $Tmc1^{Bth/+}$ mouse model carries the orthologous missense mutation (p.M412K, c.T1235A) in the mouse *Tmc1* gene and exhibits progressive elevation of the auditory response threshold and progressive hair cell loss beginning at one month of age[21]. As the orthologous mutations in human and mouse both cause progressive, profound hearing loss, the $Tmc1^{Bth/+}$ mouse is a promising model for the development of treatment strategies[21].

We began by developing a genome editing strategy that preferentially disrupts the mouse mutant $Tmc1^{Bth}$ allele. To distinguish the mutant and wild-type alleles, we identified sgRNAs that target *Tmc1* at sites that include the T1235A mutation and a nearby NGG protospacer-adjacent motif (PAM) sequence required by *Streptococcus pyogenes* Cas9. We identified three candidate sgRNAs (Tmc1-mut1, Tmc1-mut2 and Tmc1-mut3) that place the *Bth* mutation at position 11, 12, and 15, respectively, of the spacer, counting the PAM as positions 21–23 (Fig. 1a). Mismatches between the sgRNA and genomic DNA that are close to the PAM are poorly tolerated by Cas9[10], increasing the likelihood that the *Bth* mutant allele will be selectively edited. A fourth sgRNA, Tmc1-mut4, is a truncated version of Tmc1-mut3 designed to increase genome editing DNA specificity[22]. We evaluated the ability of these four sgRNAs in complex with Cas9 to cleave either the wild-type *Tmc1* or the $Tmc1^{Bth}$ allele *in vitro*. All sgRNAs tested comparably or preferentially cleaved the $Tmc1^{Bth}$ allele, with Tmc1-mut3 exhibiting the greatest selectivity (Extended Data Fig. 1a, b).

We performed lipid-mediated delivery of Cas9–sgRNA RNP complexes into cultured primary fibroblasts derived from wild-type or homozygous $Tmc1^{Bth/Bth}$ mice to evaluate the allele specificity of genomic DNA modification in mouse cells. We delivered Cas9 complexed with each of the four sgRNAs using Lipofectamine 2000 into both wild-type and $Tmc1^{Bth/Bth}$ mutant fibroblasts. RNP delivery into these primary fibroblasts was twofold to fourfold less efficient than with HEK293T cells (Extended Data Fig. 1c). The highest rate of targeted insertions and deletions (indels) in mutant $Tmc1^{Bth/Bth}$ fibroblasts (10%) was observed with Cas9–Tmc1-mut3 RNPs, while lower indel frequencies (0.74–4.1%) were observed using the other sgRNAs (Fig. 1b).

[1]Department of Chemistry and Chemical Biology, Harvard University, Cambridge, Massachusetts 02138, USA. [2]Howard Hughes Medical Institute, Harvard University, Cambridge, Massachusetts 02138, USA. [3]Broad Institute of MIT and Harvard, Cambridge, Massachusetts 02141, USA. [4]Department of Otolaryngology and Program in Neuroscience, Harvard Medical School and Eaton Peabody Laboratory, Massachusetts Eye and Ear Infirmary, Boston, Massachusetts 02114, USA. [5]Department of Otorhinolaryngology, Union Hospital, Tongji Medical College, Huazhong University of Science and Technology, Wuhan, Hubei 430022, China. [6]Program in Speech and Hearing Bioscience and Technology, Harvard University, Cambridge, Massachusetts 02138, USA. [7]Departments of Otolaryngology and Neurology, F.M. Kirby Neurobiology Center Boston Children's Hospital and Harvard Medical School, Boston, Massachusetts 02115, USA. [8]Department of Otolaryngology–Head and Neck Surgery, Eye and ENT Hospital, Shanghai Medical College, Fudan University, Shanghai, China. [9]Department of Biomedical Engineering, Tufts University, Medford, Massachusetts 02155, USA. [10]Department of Otolaryngology & Head Neck Surgery, Key Lab of Hearing Impairment Science of Ministry of Education, Key Lab of Hearing Impairment Prevention and Treatment of Beijing City, Chinese PLA Medical School, Beijing, China. †Present addresses: Department of Chemical and Biomolecular Engineering, Rice University, Houston, Texas 77005, USA (X.G.); Department of Otolaryngology-Head and Neck Surgery, Shanghai Ninth People's Hospital and Ear Institute, Shanghai Jiaotong University School of Medicine, Shanghai, 200011, China (Y.T.).
*These authors contributed equally to this work.
§These authors jointly supervised this work.

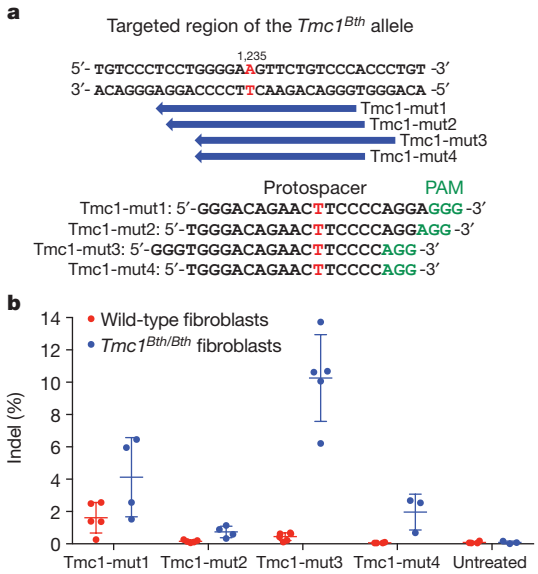

Figure 1 | Design of a genome-editing strategy to disrupt the *Tmc1*^{Bth} mutant allele. a, SpCas9 sgRNAs were designed to target the mutant *Tmc1*^{Bth} allele, in which T1235 is changed to A (red). The protospacer (blue arrows) of each *Tmc1*^{Bth}-targeting sgRNA contains a complementary T (red) that pairs with the T1235A mutation in the *Tmc1*^{Bth} allele, but that forms a mismatch with the wild-type *Tmc1* allele. **b**, Lipid-mediated delivery of Cas9–sgRNA complexes into primary fibroblasts derived from wild-type or homozygous *Tmc1*$^{Bth/Bth}$ mice. Purified Cas9 protein (100 nM) and 100 nM of each sgRNA shown were delivered using Lipofectamine 2000. Indels were quantified by HTS. Individual values ($n = 3$–6) are shown; horizontal lines and error bars represent the mean values ± s.d. of three or more independent biological replicates.

By contrast, all tested sgRNAs edited the wild-type *Tmc1* locus much less efficiently in wild-type fibroblasts (0.066–1.6% indels) (Fig. 1b). Notably, Cas9–Tmc1-mut3 modified the mutant *Tmc1*^{Bth} allele 23-fold more efficiently than the wild-type allele (Fig. 1b and Extended Data Fig. 1d). We also prepared three corresponding wild-type *Tmc1*-targeting sgRNAs (Tmc1-wt1, Tmc1-wt2 and Tmc1-wt3) that lack the T1235A mutation. These sgRNAs edited wild-type fibroblasts on average tenfold more efficiently than *Tmc1*$^{Bth/Bth}$ fibroblasts (Extended Data Fig. 1e), confirming that the observed allele selectivities did not arise from the inability of the wild-type *Tmc1* allele to be edited.

We tested 17 cationic lipids for their ability to deliver the Cas9–Tmc1-mut3 RNP into *Tmc1*$^{Bth/Bth}$ fibroblasts. Several lipids supported substantial modification of the target locus, including RNAiMAX (7.7%), CRISPRMAX (8.9%), and Lipofectamine 2000 (12%) (Extended Data Fig. 2). By contrast, treatment of wild-type fibroblasts with Cas9–Tmc1-mut3 and the same set of 17 lipids resulted in low (≤0.5%) indel rates (Extended Data Fig. 2a, b). These results suggest that the target mutant *Tmc1* locus can be preferentially disrupted by Cas9–guide RNA complexes.

Exposure of cells to Cas9–sgRNA agents typically results in the modification of both on-target and off-target loci[10,23]. We used both the GUIDE-seq method[23] and computational prediction[24] to identify potential off-target loci that could be modified by exposure to Cas9–Tmc1-mut3. Ten off-target sites containing up to six mismatches in the protospacer region of Tmc1-mut3 sgRNA were identified by GUIDE-seq (Extended Data Fig. 3a). None of these off-target loci are known to be associated with hearing function (Extended Data Table 1a). We measured the indel frequency at each off-target site by high-throughput sequencing (HTS) in *Tmc1*$^{Bth/Bth}$ primary mouse fibroblasts treated with Cas9–Tmc1-mut3 following plasmid DNA nucleofection or RNP delivery. Plasmid nucleofection resulted in 0.68–8.1% indels at nine of the ten GUIDE-seq-identified off-target sites (Extended Data Fig. 3b and Extended Data Table 1a). By contrast, after RNP delivery, modification of only one off-target site (*off-T1*, 1.2% indels) was detected (Extended Data Fig. 3b), consistent with our earlier findings that RNP delivery greatly reduces off-target editing compared with DNA delivery[15]. Among the computationally predicted off-target sites[24], only the two (*off-T1′* and *off-T2′*) that were also identified as off-targets by GUIDE-seq were observed to undergo modification (Extended Data Table 1b). Together, these results suggest that delivery of Cas9–Tmc1-mut3 RNP complexes into *Tmc1*$^{Bth/Bth}$ cells leads to minimal off-target modification, and that phenotypes affecting hearing are unlikely to arise from off-target modification.

To evaluate the ability of the Cas9–Tmc1-mut3 sgRNA complex to target the *Tmc1*^{Bth} allele in hair cells *in vivo*, we complexed Cas9–Tmc1-mut3 sgRNA with Lipofectamine 2000 and injected the resulting mixture into the scala media of neonatal mice by cochleostomy. Neonatal cochlear hair cells produce TMC1 and TMC2, both of which can enable sensory transduction. To isolate the effect of editing the *Tmc1*^{Bth} allele, we injected the Cas9–Tmc1-mut3 sgRNA–lipid complex into *Tmc1*$^{Bth/Δ}$*Tmc2*$^{Δ/Δ}$ mice[16], to avoid transduction current contributions from TMC2 or wild-type TMC1. We recorded sensory transduction currents from inner hair cells (IHCs) after injection with the Cas9–Tmc1-mut3–lipid complex, or with a control targeting an unrelated *Gfp* gene. We observed a significant decline in transduction current amplitudes in *Tmc1*$^{Bth/Δ}$*Tmc2*$^{Δ/Δ}$ mice following injection with Cas9–Tmc1-mut3–lipid complexes, consistent with disruption of the *Tmc1*^{Bth} allele in sensory hair cells *in vivo*, but not with Cas9–GFP sgRNA–lipid complexes (Fig. 2a, b).

In *Tmc1*$^{Bth/+}$*Tmc2*$^{+/+}$ mice (referred to hereafter as *Tmc1*$^{Bth/+}$ mice), IHCs undergo progressive death, followed by the outer hair cells (OHCs)[21]. To determine the effect of Cas9–Tmc1-mut3 sgRNA on *Tmc1*$^{Bth/+}$ hair cell survival, we injected Cas9–Tmc1-mut3–lipid complex into the scala media of mice on postnatal day 1 (P1) and removed the injected and uninjected cochleae after eight weeks. Uninjected ears exhibited substantial loss of IHCs and partial degeneration of OHCs (Fig. 2c, f, g) compared with wild-type ears (C3HeB/FeJ (C3H) mice, which are the genetic background of the *Tmc1*$^{Bth/+}$ mice) (Fig. 2e). In injected ears, survival of IHCs and OHCs was significantly enhanced (Fig. 2d, f, g). Stereocilia bundles were observed on surviving IHCs in injected ears, but were absent in uninjected ears in the basal and middle turns (Extended Data Fig. 4a). These results suggest that Cas9–Tmc1-mut3–lipid injection *in vivo* promotes hair cell survival in *Tmc1*$^{Bth/+}$ mice. The strong differences between treated and untreated ears suggests that sporadic disruption of *Tmc1*^{Bth} may benefit not only edited hair cells, but also surrounding hair cells, consistent with previous findings[25].

To study the effect of Cas9–Tmc1-mut3–lipid injection on cochlear function in *Tmc1*$^{Bth/+}$ mice, we measured auditory brainstem responses (ABRs), which represent the sound-evoked neural output of the cochlea, as well as distortion product otoacoustic emissions (DPOAEs), which measure the amplification provided by OHCs[21]. In uninjected ears of *Tmc1*$^{Bth/+}$ mice, we observed profound attenuation of cochlear neural responses, with ABR thresholds ranging from 70–90 dB at four weeks of age, compared with 30–50 dB for wild-type C3H mice (Fig. 3a and Extended Data Fig. 4b). The elevations in DPOAE thresholds at this time in *Tmc1*$^{Bth/+}$ mice were smaller than the elevations in ABR threshold (Extended Data Fig. 5a), consistent with reports that IHCs are more severely affected than OHCs in *Tmc1*$^{Bth/+}$ mice[21]. Four weeks after Cas9–Tmc1-mut3–lipid injection, treated *Tmc1*$^{Bth/+}$ ears showed substantially enhanced cochlear function, with lower ABR thresholds relative to uninjected ears at all frequencies below 45 kHz (Fig. 3a). Significant ($P \leq 0.001$) hearing preservation was detected from 8 to 23 kHz, with average ABR thresholds 15 dB lower for treated ears than untreated contralateral ears (Fig. 3a; Supplementary Table 1). DPOAE thresholds were slightly elevated in the injected ears, consistent with OHC damage, perhaps from the injection procedure (Extended Data Fig. 5). We also observed greater ABR wave 1 amplitudes, and a more normal

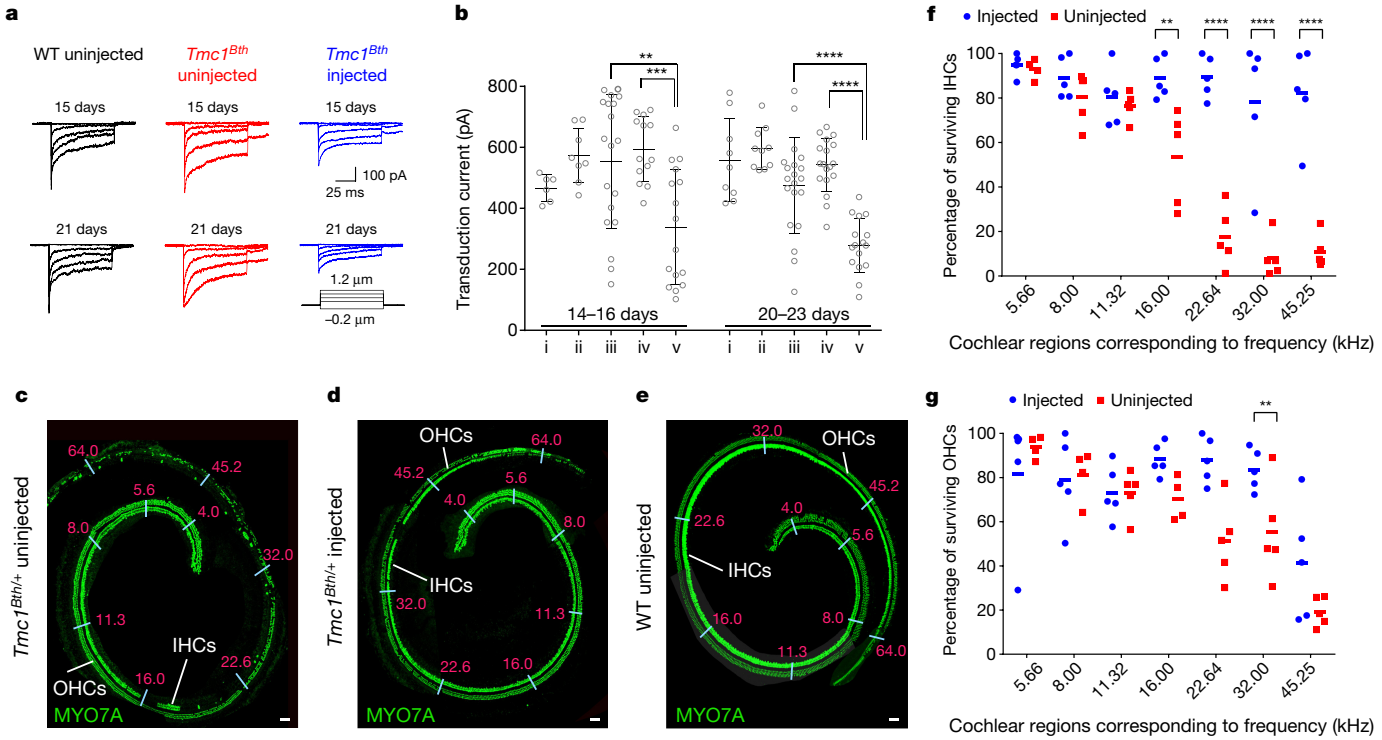

Figure 2 | Effects of Cas9–Tmc1-mut3 sgRNA–lipid injection on hair-cell function and hair-cell survival in mice. a, Representative transduction currents from IHCs of P0–P1 wild-type (WT) or $Tmc1^{Bth/\Delta}Tmc2^{\Delta/\Delta}$ mice that were uninjected, or injected with the Cas9–Tmc1-mut3–lipid complex, 15 or 21 days after injection. **b**, Maximal transduction current amplitudes for 135 IHCs from wild-type C57B/L6 and $Tmc1^{Bth/\Delta}Tmc2^{\Delta/\Delta}$ mice. i, uninjected wild-type C57B/L6 mice; ii, wild-type C57B/L6 mice injected at P1 with Cas9–Tmc1-wt3–lipid; iii, uninjected $Tmc1^{Bth/\Delta}Tmc2^{\Delta/\Delta}$ mice; iv, $Tmc1^{Bth/\Delta}Tmc2^{\Delta/\Delta}$ mice injected at P1 with Cas9–GFP sgRNA–lipid; v, $Tmc1^{Bth/\Delta}Tmc2^{\Delta/\Delta}$ mice injected at P1 with Cas9–Tmc1-mut3–lipid. Data were recorded after 14-23 days. Individual values ($n = 6$–20) are shown; horizontal lines and error bars reflect mean ± s.d. **c**–**e**, Representative confocal microscopy images around the age of eight weeks from an uninjected $Tmc1^{Bth/+}$ cochlea (**c**); the contralateral cochlea of the mouse in **c** injected with Cas9–Tmc1-mut3–lipid complex at P1 (**d**); and an untreated wild-type C3H cochlea (**e**). Numbers in pink indicate approximate frequencies (in kHz) sensed by each region. Scale bars, 50 µm. **f**, **g**, Quantification of IHC (**f**) and OHC (**g**) survival percentages in $Tmc1^{Bth/+}$ mice relative to wild-type C3H mice (100%) eight weeks after Cas9–Tmc1-mut3–lipid injection (blue) compared to uninjected (red) contralateral ears. Individual values are shown; horizontal lines represent mean values of five biological replicates. Statistical tests in **b** are two-population *t*-tests, and in **f**, **g** are two-way ANOVAs with Bonferroni correction: $^{**}P < 0.01$, $^{***}P < 0.001$, $^{****}P < 0.0001$.

ABR waveform pattern, in injected ears than in uninjected controls (Fig. 3b, c). Together, these results show that injection of neonatal $Tmc1^{Bth/+}$ mice with Cas9–Tmc1-mut3–lipid complexes reduces progressive hearing loss.

To test whether amelioration of hearing loss requires the mutant $Tmc1^{Bth}$ allele-specific sgRNA, we injected Cas9–Tmc1-wt3–lipid complexes targeting the wild-type *Tmc1* allele rather than the $Tmc1^{Bth}$ mutant allele into P1–2 $Tmc1^{Bth/+}$ mice. After four weeks, ABR thresholds in the injected ears were similar to, or worse than, those in the contralateral uninjected ears (Extended Data Fig. 6a; Supplementary Table 1), consistent with the inability of Cas9–Tmc1-wt3 to efficiently disrupt the $Tmc1^{Bth}$ allele (Extended Data Fig. 1e), and possible disruption of wild-type *Tmc1*. Injection of Cas9–sgRNA–lipid complexes targeting an unrelated gene (*Gfp*) did not significantly affect ABR thresholds at most tested frequencies in $Tmc1^{Bth/+}$ mice (Extended Data Fig. 6b). To test whether preservation of cochlear function requires Cas9 nuclease activity, rather than transcriptional interference from Cas9 binding to *Tmc1*, we treated $Tmc1^{Bth/+}$ mice with catalytically inactive dCas9[10] complexed with Tmc1-mut1 sgRNA and observed no evidence of hearing preservation (Extended Data Figs 5d, 6c; Supplementary Table 1). To evaluate the effects of the treatment on normal mice, we injected Cas9–Tmc1-mut3–lipid into wild-type C3H mice. We observed similar or slightly elevated ABR thresholds in injected ears relative to uninjected ears four weeks after treatment (Extended Data Fig. 6d, e), suggesting that Cas9–Tmc1-mut3 does not modify wild-type *Tmc1* efficiently enough to substantially affect hearing. Finally, injection of Cas9 and lipid without sgRNA did not improve ABR or DPOAE thresholds (Extended Data Fig. 6f, g). Collectively, these results establish that hearing preservation depends on sgRNA allele specificity, Cas9 DNA cleavage activity, and the presence of the $Tmc1^{Bth}$ allele. We also characterized the cochlear function of $Tmc1^{Bth/+}$ mice eight weeks after treatment. Mean ABR thresholds following Cas9–Tmc1-mut3–lipid injection remained lower than uninjected controls from 5.7–23 kHz, although the average improvement was lower than at four weeks post-treatment (Extended Data Fig. 4c, d), potentially owing to continued progressive hearing loss in the non-edited hair cells.

As a behavioural measure of hearing rescue, we assessed acoustic startle responses eight weeks after injection. In uninjected $Tmc1^{Bth/+}$ mice, no startle response was detected following stimulation at 120 dB. By contrast, significant startle responses were detected in Cas9–Tmc1-mut3–lipid-injected $Tmc1^{Bth/+}$ mice following stimulus at 110 and 120 dB (Fig. 3d and Extended Data Fig. 4e), demonstrating that hearing preservation upon treatment also preserves an acoustic behavioural reflex.

To evaluate the ability of each of the other $Tmc1^{Bth}$-targeting sgRNAs to mediate hearing rescue *in vivo*, we also injected Tmc1-mut1, Tmc1-mut2, and Tmc1-mut4 complexed with Cas9 into neonatal $Tmc1^{Bth/+}$ cochleae, and observed varying degrees of enhanced cochlear function (Extended Data Fig. 7). Thus, while Tmc1-mut3 resulted in the most robust hearing preservation, other sgRNAs targeting the mutant *Bth* allele also partially preserved cochlear function.

To test whether RNP delivery of editing agents in adult mouse inner ears supports genome editing in hair cells, we injected Cas9–GFP sgRNA–lipid complexes into the cochleae of six-week-old Atoh1–GFP

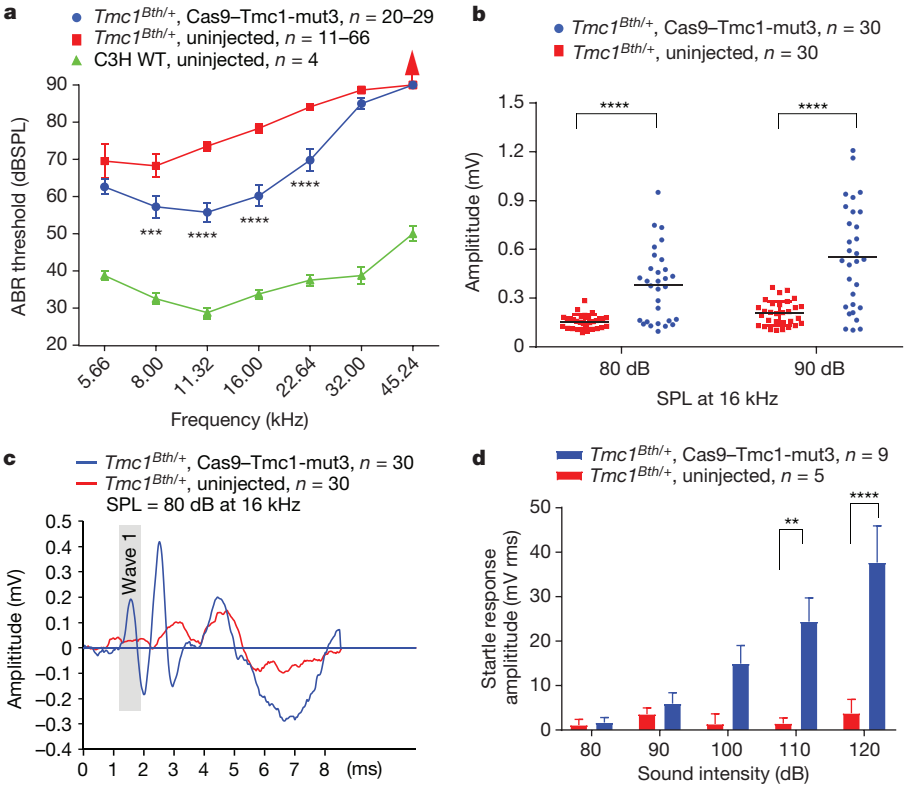

Figure 3 | Cas9–Tmc1-mut3–lipid injections reduce hearing loss in *Tmc1*$^{Bth/+}$ mice. a, ABR thresholds in *Tmc1*$^{Bth/+}$ ears injected with Cas9–Tmc1-mut3–lipid (blue), uninjected *Tmc1*$^{Bth/+}$ ears (red), and wild-type C3H ears (green) after four weeks. **b**, Peak amplitudes of ABR wave 1 at 16 kHz in Cas9–Tmc1-mut3–lipid-injected ears (blue) compared with uninjected ears (red) after four weeks. Horizontal bars are mean values. **c**, Mean ABR waveforms in Cas9–Tmc1-mut3–lipid-injected ears (blue) and uninjected ears (red). **d**, Startle responses in Cas9–Tmc1-mut3–lipid-injected mice (blue) and in uninjected mice (red) eight weeks after treatment. Red arrow in **a** indicates no ABR response at the highest stimulus level tested (90 dB). Statistical tests were two-way ANOVA with Bonferroni correction for multiple comparisons: $^{**}P < 0.01$, $^{***}P < 0.001$, $^{****}P < 0.0001$. Values and error bars reflect mean ± s.e.m. Among the different frequencies assayed, the number of ears tested (*n*) varies within the range shown (Supplementary Table 2).

mice by canalostomy. Two weeks after injection, loss of GFP fluorescence in the apical turn suggested target gene disruption with 25 ± 2.1% efficiency (Extended Data Fig. 8), comparable to previous observations of 20% GFP editing in neonatal hair cells[15]. These results suggest that this approach may be applicable to dominant genetic deafness that manifests with late-onset hearing loss.

To confirm that *in vivo* treatment of *Tmc1*$^{Bth/+}$ mice with Cas9–Tmc1-mut3 sgRNA disrupted the *Tmc1*^{Bth} allele, we sequenced DNA from cochlea tissue collected from injected *Tmc1*$^{Bth/+}$ and untreated *Tmc1*$^{Bth/+}$ mice. After injection on P1, tissues were removed on P5 and separated into organ of Corti (containing hair cells), spiral ganglion, and spiral ligament samples (Extended Data Fig. 9a, b). We estimated the fraction of hair cells in dissected cochlear tissue to be only about 1.5% of the total cells used for DNA sequencing (Extended Data Fig. 9a, b). Nevertheless, we observed unambiguous indels at the *Tmc1*^{Bth} locus in cochlear tissue from treated mice (Fig. 4a). The organ of Corti samples contained, on average, *Tmc1* editing of 0.92% of total sequenced DNA, which corresponds to about 1.8% *Tmc1*^{Bth} allele disruption in the heterozygous mice (Fig. 4a). We also isolated samples of much smaller numbers of cells (up to a few dozen, mostly hair cells) from

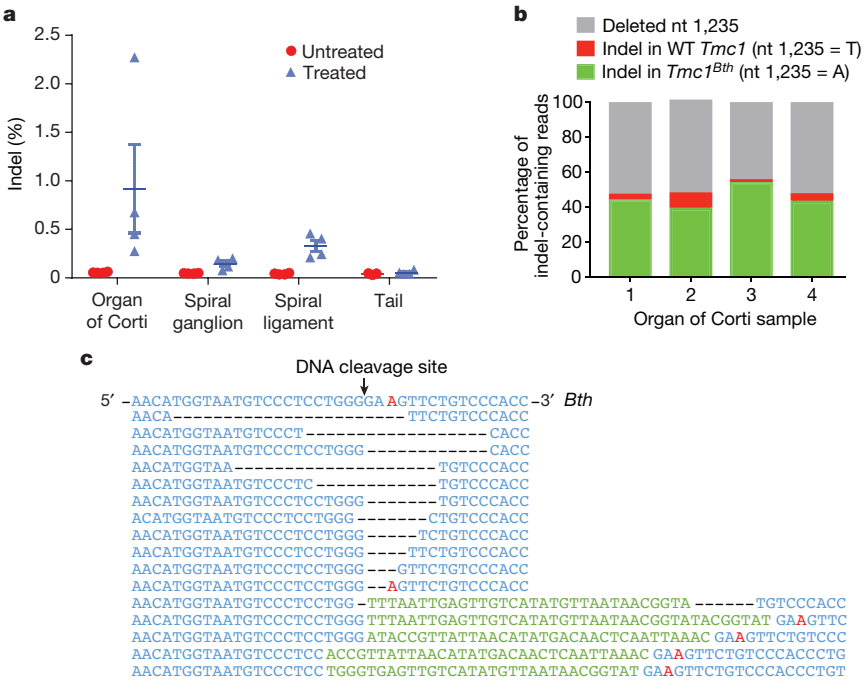

Figure 4 | Genome modification at *Tmc1* induced by lipid-mediated delivery of Cas9–Tmc1-mut3 RNP into *Tmc1*$^{Bth/+}$ mice. a, *Tmc1* indel frequencies from tissue samples four days after injection of Cas9–Tmc1-mut3–lipid (blue) or from uninjected mice (red). Individual values ($n = 4$) are shown; horizontal lines and error bars reflect mean ± s.e.m. Note that *Tmc1*^{Bth} allele editing frequencies in these heterozygous mice are approximately double the observed indel frequencies. **b**, Analysis of indel-containing *Tmc1* sequencing reads from four injected organ of Corti samples in **a**. **c**, The most abundant 16 *Tmc1* sequences, grouped by similarity, from organ of Corti samples in **b**. The T1235A *Tmc1*^{Bth} mutation is shown in red.

treated mice. Decreasing the number of cells entering the genomic DNA amplification and sequencing process increased the observed editing percentage to as high as 10% *Tmc1*^{Bth} allele disruption, but also elevated background *Tmc1* indel rates of untreated mice to an average of $0.82 \pm 0.57\%$ and a maximum of 1.6%, probably reflecting increased noise from processing of minute quantities of genomic DNA. No indel frequencies above that of untreated controls at any of the above-identified off-target sites were observed in Cas9–Tmc1-mut3–lipid-treated tissues (Extended Data Fig. 9c). Together, these observations confirm that Cas9–Tmc1-mut3–lipid treatment *in vivo* edits the *Tmc1* locus with no detected editing at GUIDE-seq-identified off-target loci.

An analysis of indel-containing *Tmc1* sequencing reads from treated *Tmc1*$^{Bth/+}$ mice allowed us to directly assess the allele specificity of Cas9–Tmc1-mut3 *in vivo*. Of 11,694 sequencing reads containing indels from four treated organ of Corti samples, 6,118 (52%) contained an intact nucleotide at *Tmc1* position 1,235. Of these, 5,736 (94%) contained modification of the mutant *Tmc1*^{Bth} allele, whereas only 382 (6%) contained modification of the wild-type *Tmc1* allele (Fig. 4b). Therefore, samples after treatment on average contained 15-fold higher modification of the *Tmc1*^{Bth} allele over the wild-type allele (Fig. 4b, c). These results demonstrate selective disruption of the *Tmc1*^{Bth} allele in *Tmc1*$^{Bth/+}$ mice, consistent with observed hearing phenotypes, even though the *Tmc1*^{Bth} and wild-type *Tmc1* alleles differ only at a single base pair.

This work shows that cationic lipid-mediated Cas9–sgRNA complex delivery *in vivo* can achieve allele-specific gene disruption in a mouse model of a human genetic disease, resulting in amelioration of the disease phenotype. Our results suggest that this approach has potential for the treatment of autosomal-dominant hearing loss related to hair cell dysfunction, and provide a complementary strategy to other approaches that use antisense oligos (ASOs) or RNA interference[6,25]. The genome editing strategy developed here may inform the future development of a DNA-free, virus-free, one-time treatment for certain genetic hearing loss disorders.

Online Content Methods, along with any additional Extended Data display items and Source Data, are available in the online version of the paper; references unique to these sections appear only in the online paper.

Received 4 April; accepted 24 November 2017.
Published online 20 December 2017.

1. Angeli, S., Lin, X. & Liu, X. Z. Genetics of hearing and deafness. *Anat. Rec. (Hoboken)* **295,** 1812–1829 (2012).
2. Marazita, M. L. *et al.* Genetic epidemiological studies of early-onset deafness in the U.S. school-age population. *Am. J. Med. Genet.* **46,** 486–491 (1993).
3. Morton, C. C. & Nance, W. E. Newborn hearing screening—a silent revolution. *N. Engl. J. Med.* **354,** 2151–2164 (2006).
4. Géléoc, G. S. & Holt, J. R. Sound strategies for hearing restoration. *Science* **344,** 1241062 (2014).
5. Müller, U. & Barr-Gillespie, P. G. New treatment options for hearing loss. *Nat. Rev. Drug Discov.* **14,** 346–365 (2015).
6. Shibata, S. B. *et al.* RNA interference prevents autosomal-dominant hearing loss. *Am. J. Hum. Genet.* **98,** 1101–1113 (2016).
7. Pan, B. *et al.* Gene therapy restores auditory and vestibular function in a mouse model of Usher syndrome type 1c. *Nat. Biotechnol.* **35,** 264–272 (2017).
8. Ahmed H., Shubina-Oleinik O. & Holt, J. R. Emerging gene therapies for genetic hearing loss. *J. Assoc. Res. Otolaryngol.* **18,** 649–670 (2017).
9. Sacheli, R., Delacroix, L., Vandenackerveken, P., Nguyen, L. & Malgrange, B. Gene transfer in inner ear cells: a challenging race. *Gene Ther.* **20,** 237–247 (2013).
10. Komor, A. C., Badran, A. H. & Liu, D. R. CRISPR-based technologies for the manipulation of eukaryotic genomes. *Cell* **168,** 20–36 (2017).
11. Long, C. *et al.* Postnatal genome editing partially restores dystrophin expression in a mouse model of muscular dystrophy. *Science* **351,** 400–403 (2016).
12. Yang, Y. *et al.* A dual AAV system enables the Cas9-mediated correction of a metabolic liver disease in newborn mice. *Nat. Biotechnol.* **34,** 334–338 (2016).
13. Yin, H. *et al.* Therapeutic genome editing by combined viral and non-viral delivery of CRISPR system components *in vivo*. *Nat. Biotechnol.* **34,** 328–333 (2016).
14. Kim, S., Kim, D., Cho, S. W., Kim, J. & Kim, J. S. Highly efficient RNA-guided genome editing in human cells via delivery of purified Cas9 ribonucleoproteins. *Genome Res.* **24,** 1012–1019 (2014).
15. Zuris, J. A. *et al.* Cationic lipid-mediated delivery of proteins enables efficient protein-based genome editing *in vitro* and *in vivo*. *Nat. Biotechnol.* **33,** 73–80 (2015).
16. Pan, B. *et al.* TMC1 and TMC2 are components of the mechanotransduction channel in hair cells of the mammalian inner ear. *Neuron* **79,** 504–515 (2013).
17. Camp, G. V. & Smith, R. *Hereditary Hearing Loss Homepage* http://hereditaryhearingloss.org (2017).
18. Zhao, Y. *et al.* A novel DFNA36 mutation in TMC1 orthologous to the Beethoven (Bth) mouse associated with autosomal dominant hearing loss in a Chinese family. *PLoS One* **9,** e97064 (2014).
19. Kurima, K. *et al.* Dominant and recessive deafness caused by mutations of a novel gene, TMC1, required for cochlear hair-cell function. *Nat. Genet.* **30,** 277–284 (2002).
20. Kawashima, Y., Kurima, K., Pan, B., Griffith, A. J. & Holt, J. R. Transmembrane channel-like (TMC) genes are required for auditory and vestibular mechanosensation. *Pflugers Arch.* **467,** 85–94 (2015).
21. Vreugde, S. *et al.* Beethoven, a mouse model for dominant, progressive hearing loss DFNA36. *Nat. Genet.* **30,** 257–258 (2002).
22. Fu, Y., Sander, J. D., Reyon, D., Cascio, V. M. & Joung, J. K. Improving CRISPR-Cas nuclease specificity using truncated guide RNAs. *Nat. Biotechnol.* **32,** 279–284 (2014).
23. Tsai, S. Q. *et al.* GUIDE-seq enables genome-wide profiling of off-target cleavage by CRISPR-Cas nucleases. *Nat. Biotechnol.* **33,** 187–197 (2015).
24. Zhang, F. *CRISPR Design* http://crispr.mit.edu (2015).
25. Lentz, J. J. *et al.* Rescue of hearing and vestibular function by antisense oligonucleotides in a mouse model of human deafness. *Nat. Med.* **19,** 345–350 (2013).

Supplementary Information is available in the online version of the paper.

Acknowledgements This work was supported by DARPA HR0011-17-2-0049 (to D.R.L.), US NIH R01 EB022376 (to D.R.L.), R35 GM118062 (to D.R.L.), R01 DC006908 (to Z.-Y.C), P30 DC05209 (to M.C.L.), R01 DC00138 (to M.C.L.), and R01 DC013521 (to J.R.H.). We are grateful for support from the David-Shulsky Foundation (to Z.-Y.C.), a Frederick and Ines Yeatts Hair Cell Regeneration grant (to Y.T., V.L., M.H., and Y.S.), the Bertarelli Foundation and the Jeff and Kimberly Barber Fund (to J.R.H.), the Broad Institute (to D.R.L and Z.-Y.C.), and the HHMI (to D.R.L.). We thank H. Rees, S. Tsai, M. Packer, K. Zhao and D. Usanov for assistance.

Author Contributions X.G. and Y.T. designed the research, performed genome editing (X.G.) and hearing biology (Y.T.) experiments, analysed data, and wrote the manuscript. V.L., M.H., W.-H.Y., B.P., Y.-J.H., and H.W. designed experiments, performed hearing biology experiments and analysed data. D.B.P., M.C.L., and W.-J.K. designed hearing experiments and analysed data. Y.S. and S.Y. supported hearing biology experiments. J.H.H. analysed GUIDE-seq data. D.B.T. supported genome editing experiments. Y.L. and Q.X. designed and synthesized lipids. J.R.H., Z.-Y.C. and D.R.L. designed and supervised the research, and wrote the manuscript. All authors edited the manuscript.

Author Information Reprints and permissions information is available at www.nature.com/reprints. The authors declare competing financial interests: details are available in the online version of the paper. Readers are welcome to comment on the online version of the paper. Publisher's note: Springer Nature remains neutral with regard to jurisdictional claims in published maps and institutional affiliations. Correspondence and requests for materials should be addressed to D.R.L. (drliu@fas.harvard.edu) and Z.Y.C. (Zheng-Yi_Chen@meei.harvard.edu).

METHODS

Primary cell culture. Wild-type, *Tmc1*$^{Bth/+}$ and *Tmc1*$^{Bth/Bth}$ fibroblasts were obtained from P5 pups (see below). Mice were euthanized and cleaned with 70% ethanol. Underarm skin fragments (1–2 cm^2) were excised and submerged in cold HBSS (ThermoFisher). Subcutaneous fat was removed by forceps. Skin fragments were cut into ~1-mm^2 pieces with a 25G 5/8″ syringe (1180125058, Covidien). Tissues were digested with 0.5 mg/ml Liberase DL (Sigma 5401160001) at 37 °C for 1 h with occasional pipetting up and down to break cell clumps. Warm culture medium (1:1 DMEM:F12 medium (ThermoFisher) with 15% fetal bovine serum (FBS) (ThermoFisher) and 100 U/ml penicillin+streptomycin (ThermoFisher) was added to stop the enzyme digestion. The solution was filtered with a 70-μm cell strainer (Falcon) and centrifuged at 200*g* for 5 min. The pellet was resuspended in culture medium and transferred to a 25-ml culture flask, then incubated at 37 °C with 5% CO_2 and 3% O_2. Fibroblasts were cultured for about 2–3 days to reach ~90% confluence, then passaged in 100-ml flasks in DMEM plus GlutaMax (ThermoFisher) supplemented with 10% (v/v) FBS at 37 °C with 5% CO_2.

Delivery of proteins complexed with cationic lipids into mouse fibroblasts. Cultured fibroblast cells were plated in 24-well format (500 μl well volume) in Dulbecco's modified Eagle's medium plus GlutaMAX (DMEM, Life Technologies) with 10% FBS (no antibiotics) at a cell density sufficient to reach ~80% confluence at the time of usage. Purified sgRNA was incubated with Cas9 protein for 5 min before complexing with cationic lipid[15,26]. Delivery of Cas9–sgRNA was performed by combining 100 nM RNP complex with 3 μl cationic lipid in 50 μl OPTIMEM medium (Life Technologies) according to the manufacturer's protocol for DNA plasmid transfection. The above mixture containing cationic lipid and RNP was then added to cells. All complexing steps were performed at room temperature. Cells were harvested and genomic DNA was extracted for sequencing ~96 h after treatment.

GUIDE-seq and data analysis. Mouse fibroblasts were transfected using 1,000 ng Cas9 plasmid (pCas9), 300 ng sgRNA plasmid (pTmc1-mut3 sgRNA), and 50 pmol GUIDE-seq double-stranded oligodeoxynucleotides (dsODN) using a LONZA 4D-Nucleofector. Transfection programs were optimized following the manufacturer's instructions (CA158 and CA189, P2 Primary Cell 4D-Nucleofector X Kit). pmaxGFP Control Vector (400 ng; LONZA) was added to the nucleofection solution to assess nucleofection efficiency in primary cells. The medium was replaced ~16 h after nucleofection and cells were collected for genomic DNA extraction after ~96 h. For GUIDE-seq off-target DNA cleavage analysis, pCas9, pTmc1-mut3 sgRNA, pmaxGFP, and dsODN were nucleofected into *Tmc1*$^{Bth/+}$ heterozygous mouse primary fibroblasts. A sample nucleofected with dsODN only served as a negative control. About 400 ng genomic DNA for each sample was sheared acoustically using a Covaris m220 sonicator to an average length of 500 bp in 130 μl TE buffer. Each sample was sequenced on an Illumina Miseq following previously described protocols[23]. Reads were consolidated first by their Illumina indexes and then by the 8-nt molecular index that defines a single pre-PCR template fragment. The consolidated reads were mapped to the mouse reference genome (GRCm38) using BWA-MEM. Off-target sites were identified by first mapping the start position of the amplified sequences using a 10-bp sliding window, then retrieving the reference sequence around the site. Given the size of some of the deletions, the number of base pairs used as the flanking sequence was increased to 100 bp. The retrieved sequences were aligned to the Cas9 target sequence using a Smith–Waterman local-alignment algorithm.

High-throughput DNA sequencing of genomic DNA samples. Treated cells or tissues were collected after four days and genomic DNA was isolated using the Agencourt DNAdvance Genomic DNA Isolation Kit (Beckman Coulter) according to the manufacturer's instructions. On-target and off-target genomic regions of interest were amplified by PCR with flanking HTS primer pairs (listed in Supplementary Sequences). PCR amplification was carried out with Phusion high-fidelity DNA polymerase (ThermoFisher) according to the manufacturer's instructions using ~100 ng genomic DNA as a template. PCR cycle numbers were chosen to ensure the reaction was stopped during the log-linear range of amplification. PCR products were purified using RapidTips (Diffinity Genomics). Purified DNA was amplified by PCR with primers containing sequencing adaptors. The products were purified by gel electrophoresis and quantified using the Quant-iT^{TM} PicoGreen dsDNA Assay Kit (ThermoFisher) and KAPA Library Quantification Kit-Illumina (KAPA Biosystems). Samples were sequenced on an Illumina MiSeq as previously described[27].

Sequencing reads were demultiplexed using MiSeq Reporter (Illumina), and individual FASTQ files were analysed with a custom Matlab script (Supplementary Note). Each read was pairwise aligned to the appropriate reference sequence using the Smith–Waterman algorithm. Base calls with a *Q*-score below 31 were excluded from calculating editing frequencies. Sequencing reads were scanned for exact matches to two 10-bp sequences that flank both sides of a window in which indels might occur. If no exact matches were located, the read was excluded from analysis. If the length of this indel window exactly matched the reference sequence, the read was classified as not containing an indel. If the indel window was one or more bases longer or shorter than the reference sequence, then the sequencing read was classified as an insertion or deletion, respectively.

General *in vivo* experiments. All *in vivo* experiments were carried out in accordance with NIH guidelines for the care and use of laboratory animals and were approved by the Massachusetts Eye & Ear Infirmary IACUC committee. Isogenic heterozygous *Tmc1*$^{Bth/+}$ mice maintained on a C3HeB/FeJ (C3H) background were obtained as a gift from A. Griffith[21], and inbred with wild-type C3H mice obtained from Jackson Laboratory. Crossbred homozygous C3H-*Tmc1*$^{Bth/Bth}$ mice were caged with C3H mice to generate heterozygous *Tmc1*$^{Bth/+}$ mice. All mice were genotyped by Transnetyx. For mechanotransduction experiments, two genotypes of *Tmc* mutant mice: *Tmc1*$^{Bth/Bth}$*Tmc2*$^{\Delta/\Delta}$ and *Tmc1*$^{\Delta/\Delta}$*Tmc2*$^{\Delta/\Delta}$[16], were bred to generate *Tmc1*$^{Bth/\Delta}$*Tmc2*$^{\Delta/\Delta}$ mice.

Microinjection into the inner ear of neonatal mice. A total of 106 *Tmc1*$^{Bth/+}$ or C3H mice (P0–2) of either sex were used for injections. The mice were randomly assigned to the different experimental groups. The final 25% of the experiments were performed in a double-blinded manner. At least five mice were injected in each group. All surgical procedures were done in a clean, dedicated space. Instruments were thoroughly cleaned with 70% ethanol and autoclaved before surgery. Fresh Cas9 and sgRNA were mixed before injection at a final concentration of 25 μM. One microlitre Lipofectamine 2000 was mixed with 1 μl Cas9–sgRNA RNP and incubated for 20 min at room temperature. Mice were anaesthetized by hyperthermia on ice. Cochleostomy was performed by preauricular incision to expose the cochlear bulla. Anatomical landmarks included the stapedial artery and tympanic ring, which were identified before injection. Glass micropipettes (4878, WPI) were pulled with a micropipette puller (PP83, Narishige) to a final outer diameter of ~10 μm. Needles held by a Nanolitre 2000 micromanipulator (WPI) were used to manually deliver the Cas9–sgRNA–lipid complexes into the scala media, which allows access to inner ear cells. The injection sites were the base, middle, and apex–middle turn of the cochlea. The volume for each injection was 0.3 μl with a total volume of 0.9 μl per cochlea. The release rate was 69 nl/min, controlled by a MICRO4 microinjection controller (WPI).

Microinjection into adult inner ear by canalostomy. Three 6-week-old Atoh1–GFP mice[28] were injected with Cas9–GFP sgRNA–lipid complex, with the same concentration and volume for each component as used in injection into neonatal inner ear. Mice were anaesthetized by intraperitoneal injection of xylazine (10 mg/kg) and ketamine (100 mg/kg). The right post-auricular region was exposed by shaving and disinfected with 10% povidone iodine. For canalostomy, a 10-mm postauricular incision was made under the operating microscope, and the right pinna and the sternocleidomastoid muscle were extracted to expose the posterior semicircular canal (PSCC), located in the margin of the temporal bone. We used a Bonn microprobe (Fine Science Tools) to drill a small hole on the PSCC, then left it open for a few minutes until no obvious perilymph leakage was observed. The tip of the polyimide tube (inner diameter 0.0039 inches, outer diameter 0.0049 inches, Microlumen) was inserted into the PSCC towards the ampulla. The hole was sealed with tissue adhesive (3M Vetbond), and a lack of fluid leakage indicated the tightness of the sealing. The tubing was cut after injection, with approximately 5 mm of tubing left connected to the PSCC and sealed with tissue adhesive. The volume for each injection was 1 μl per cochlea. The release rate was 169 nl/min, controlled by MICRO4 microinjection controller (WPI). The skin was closed with 5-0 nylon suture (Ethicon Inc.). The total surgery time was approximately 20 min, including a 6-min injection period.

Acoustic testing. ABR and DPOAE were recorded as described previously[29] at 32 °C in a soundproof chamber. Mice of either sex were anaesthetized with xylazine (10 mg/kg, intraperitoneally (i.p.)) and ketamine (100 mg/kg, i.p.). Acoustic stimuli were delivered through a custom acoustic assembly consisting of two miniature dynamic electrostatic earphones (CDMG15008-03A, CUI) to generate primary tones and a miniature microphone (FG-23329-PO7, Knowles) to record ear-canal sound pressure near the eardrum. Custom LabVIEW software controlling National Instruments 24-bit soundcards (6052E) generated all ABR and DPOAE stimuli and recorded all responses.

For ABR measurements, needle electrodes were inserted at the vertex and ventral edge of the pinna, with a ground reference near the tail. ABR potentials were evoked with 5-ms tone pips (0.5-ms rise–fall with a cos2 onset, delivered at 35/s). The response was amplified 10,000-fold, filtered (100 Hz–3 kHz passband), digitized, and averaged (1,024 responses) at each SPL. The sound level was raised in 5 dB steps from 30 dB below threshold up to 90 dB SPL at frequencies from 5.66-45.24 kHz (in half-octave steps). Following visual inspection of stacked waveforms, "threshold" was defined as the lowest sound pressure level (SPL) at which any wave could be detected. In general, thresholds were defined by three

independent observers. Wave 1 amplitude was defined as the difference between the average of the 1-ms pre-stimulus baseline and the wave 1 peak (P1), after additional high-pass filtering to remove low-frequency baseline shifts.

For DPOAE measurements, the cubic distortion product was measured in response to primaries $f1$ and $f2$. The primary tones were set so that the frequency ratio ($f2/f1$) was 1.2 and so that the $f2$ level was 10 dB below the $f1$ level. For each $f2/f1$ primary pair, primaries were swept in 5-dB steps from 20 dB SPL to 80 dB SPL (for $f2$). At each level, the amplitude of the DPOAE at $2f1–f2$ was extracted from the averaged spectra, along with the noise floor. Threshold was computed by interpolation as the $f2$ level required to produce a DPOAE at 5 dB SPL.

Acoustic startle reflex. Mice were placed into a small, acoustically transparent cage resting atop a piezoelectric force plate in a sound attenuated booth. Acoustic stimuli and amplified force plate signals were encoded by a digital signal processor (Tucker-Davis Technologies, RX6) using LabView scripts (National Instruments). Mice were placed in silence for 2 min and 60 dB broadband white noise for 5 min to acclimate to the test environment before real measurements. Broadband white noise was presented at a background level of 60 dB SPL throughout the experiment and a 16-kHz tone was presented at randomized intervals from an overhead speaker (80 dB to 120 dB SPL, 20 ms duration with 0 ms onset and offset ramps). Ten repetitions were recorded for each of the intensities per test subject. Startle response amplitude was measured as the root mean square (RMS) voltage of the force plate signal shortly after sound presentation.

Immunohistochemistry and histology. Injected and non-injected cochleae were removed after animals were killed by CO_2 inhalation. Temporal bones were fixed in 4% paraformaldehyde at 4 °C overnight, then decalcified in 120 mM EDTA for at least 1 week. The cochleae were dissected in pieces from the decalcified tissue for whole-mount immunofluorescence. Tissues were infiltrated with 0.3% Triton X-100 and blocked with 8% donkey serum for 1 h before applying the first antibody. Rabbit anti-MYO7A (1:500 ; #25-6790, Proteus BioSciences), chicken anti-GFP (1:750; ab13970, Abcam) and goat anti-SOX2 (1:350; sc-17320, Santa Cruz Biotechnology) were used at room temperature overnight. The second antibody was incubated for 1 h after three rinses with PBS rinses. All Alexafluor secondary antibodies were from Invitrogen: donkey anti-rabbit Alex488 (A21206) or Alex 594 (A21207), donkey anti goat Alex594 (A11058) or Alexa-488-phalloidin (A12379) and goat anti-chicken Alex488 (A-11039) were used at a 1:500 dilution. Specimens were mounted in ProLong Gold Antifade Mountant medium (P36930, Life Technologies). Confocal images were taken with a Leica TCS SP5 microscope using a 20× or 63× glycerin-immersion lens, with or without digital zoom. For IHC and OHC counting, we acquired z-stacks by maximum intensity projections of z-stacks for each segment by imageJ (NIH image), and composite images showing the whole cochlea were constructed in Adobe Photoshop CS3 to show the whole turn of cochlea. A frequency map was constructed for each case by measuring the spiral extent of all the dissected cochlear pieces and converting cochlear location to frequency using a plug-in of ImageJ (https://www.masseyeandear.org/research/otolaryngology/investigators/laboratories/eaton-peabody-laboratories/epl-histology-resources/imagej-plugin-for-cochlear-frequency-mapping-in-whole-mounts). MYO7A-positive IHCs and OHC were counted in the cochlear regions that respond to different sound frequencies, and any segments containing dissection-related damage were omitted from further analysis.

Hair cell transduction current recording. Wild-type or $Tmc1^{Bth/\Delta}Tmc2^{\Delta/\Delta}$ littermates were injected with 0.9 µl Cas9–Tmc1-mut3–Lipofectamine 2000 or Cas9–GFP sgRNA–Lipofectamine 2000. Wild-type C57B/L6 mice were injected with 0.9 µl Cas9–Tmc1-wt3–Lipofectamine 2000 at P0–P1 via cochleostomy. Cochleae were removed at P5–P6 and cultured in MEM(1×) + GlutaMAX-I medium with 1% FBS at 37 °C, 5% CO_2 for up to 15 days. For recording, the organs of Corti were bathed in standard artificial perilymph containing 137 mM NaCl, 0.7 mM NaH_2PO_4, 5.8 mM KCl, 1.3 mM $CaCl_2$, 0.9 mM $MgCl_2$, 10 mM HEPES, and 5.6 mM D-glucose. Vitamins (1:50) and amino acids (1:100) were added to the solution from concentrates (Invitrogen, ThermoFisher Scientific), and NaOH was used to adjust the final pH to 7.4 (~310 mOsm/kg). Recording pipettes (2–4 MΩ) were pulled from R6 capillary glass (King Precision Glass) and filled with intracellular solution containing 135 mM CsCl, 5 mM HEPES, 5 mM EGTA, 2.5 mM $MgCl_2$, 2.5 mM Na_2-ATP, and 0.1 mM $CaCl_2$; CsOH was used to adjust the final pH to 7.4 (~285 mOsm/kg). Whole-cell, tight-seal, voltage-clamp recordings were conducted at −84 mV at room temperature (22–24 °C) with an Axopatch 200B amplifier (Molecular Devices). Hair bundles were deflected with a stiff glass probe fabricated from capillary glass with a fire polisher (MF-200, World Precision Instruments) to create a rounded probe tip of ~3–5 µm in diameter. Probes were mounted on a PICMA Chip piezo actuator (Physik Instrument) and driven by an LVPZT amplifier (E-500.00, Physik Instrumente). Sensory-transduction currents were recorded from uninjected and Cas9–sgRNA-treated hair cells. The data were filtered at 10 kHz with a low-pass Bessel filter and digitized at >20 kHz with a 16-bit acquisition board (Digidata 1440A, Molecular Devices) and pClamp 10 software (Molecular Devices).

Inner ear tissue dissection for HTS. $Tmc1^{Bth/+}$ mice were injected with Cas9–sgRNA at P1 as described above. All dissection instruments were thoroughly cleaned with 70% ethanol and DRNAase Free (D6002, ARgos), then autoclaved before dissection. Mice were euthanized at P5. Temporal bones were removed and immersed in clean PBS pH 7.4 (10010001, ThermoFisher) individually. Different forceps were used for each ear. The organ of Corti, spiral ganglion, and spiral ligament from the injected and non-injected ear, and tail tissue were all removed under microscope from each mouse.

Hair cells isolation for HTS. $Tmc1^{Bth/+}$ mice were injected with Cas9–Tmc1-mut3–Lipofectamine 2000 at P1 and euthanized at P5. Cochleae were dissected and immersed in 1 µM FM 1-43FX (PA1-915, ThermoFisher) dissolved in HBSS (ThermoFisher) for 10 s at room temperature in the dark. Cochleae were rinsed three times with HBSS and placed in 100 µl Cell Recovery Solution (354253, Discovery Labware) for 10 min at 37 °C, then transferred to 100 µl TrypleE Express Enzyme (12604013, ThermoFisher). Sensory epithelia were extracted by forceps. After incubation for 10 min at 37 °C, the tissues were pipetted up and down 30 times. FM 1-43-positive cells were isolated using a 1-µl pipette under a microscope (Axiovert 200M, Carl Zeiss), then subjected to whole-genome amplification by MALBAC Single Cell WGA Kit (YK001A, Yikon Genomics).

Statistical analysis. Statistical analyses were performed by two-way ANOVA with Bonferroni corrections for multiple comparisons for ABRs, DPOAEs, and acoustic startle response; and by Student's t-test for hair cell transduction currents using Prism 6.0 (GraphPad). No statistical methods were used to predetermine sample size. A total of 106 $Tmc1^{Bth/+}$ or C3H mice (P0–2) of either sex were used for injections. The mice were randomly assigned to the different experimental groups. The final 25% of the experiments were performed in a double-blinded manner.

Code availability. Labview software for cochlear function testing is available here: http://www.masseyeandear.org/research/otolaryngology/investigators/laboratories/eaton-peabody-laboratories/epl-engineering-resources. Matlab scripts used to quantify the acoustic startle response are available from the corresponding authors on request. Indel identification scripts are provided in the Supplementary Information.

Data availability. High-throughput sequencing data have been deposited in the NCBI Sequence Read Archive database under accession code SRP103108. All other data are available from the corresponding authors on reasonable request.

26. Wang, M. *et al.* Efficient delivery of genome-editing proteins using bioreducible lipid nanoparticles. *Proc. Natl Acad. Sci. USA* **113,** 2868–2873 (2016).
27. Pattanayak, V. *et al.* High-throughput profiling of off-target DNA cleavage reveals RNA-programmed Cas9 nuclease specificity. *Nat. Biotechnol.* **31,** 839–843 (2013).
28. Lumpkin, E. A. *et al.* Math1-driven GFP expression in the developing nervous system of transgenic mice. *Gene Expr. Patterns* **3,** 389–395 (2003).
29. Huang, M., Kantardzhieva, A., Scheffer, D., Liberman, M. C. & Chen, Z. Y. Hair cell overexpression of Islet1 reduces age-related and noise-induced hearing loss. *J. Neurosci.* **33,** 15086–15094 (2013).

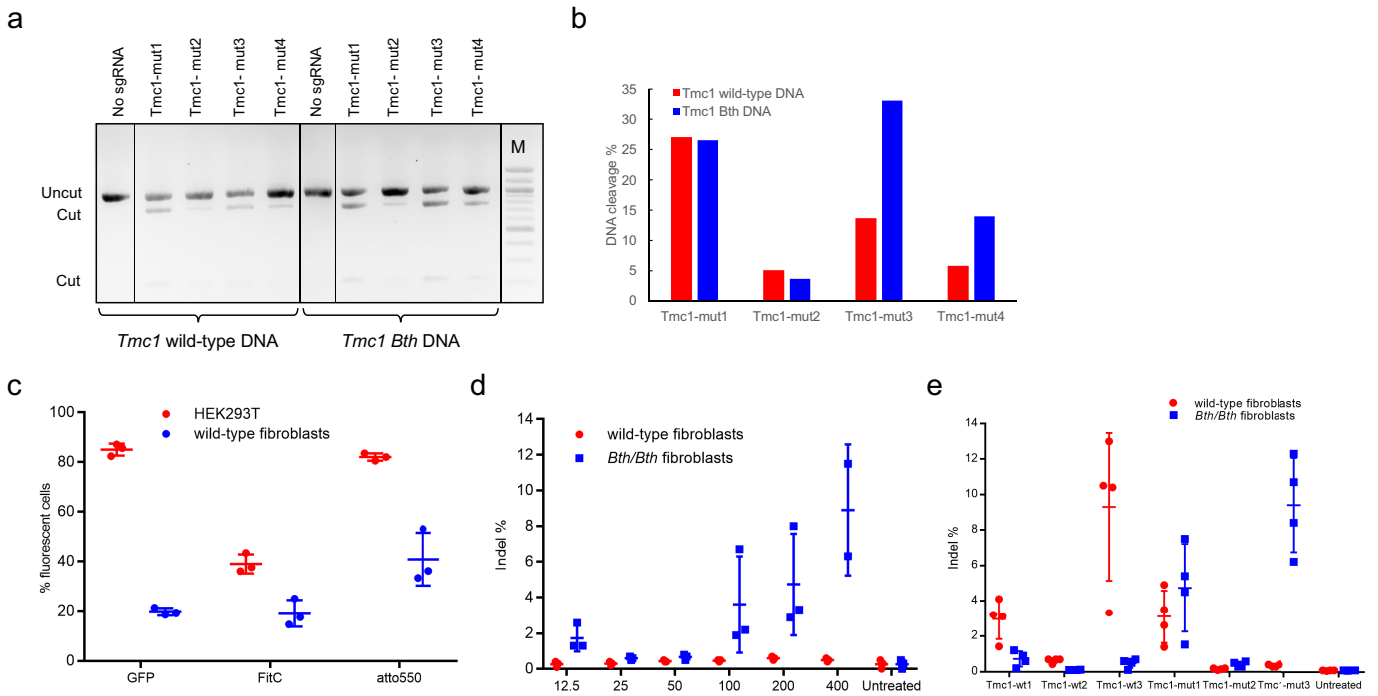

Extended Data Figure 1 | Allele-selective editing of wild-type or *Bth* mutant *Tmc1* in cleavage assays *in vitro* and by lipid-mediated delivery into primary fibroblasts. a, *In vitro* Cas9–sgRNA-mediated *Tmc1* DNA cleavage. We incubated 100 nM of a 995-bp DNA fragment containing wild-type *Tmc1* (lanes 1–5) or $Tmc1^{Bth}$ (lanes 6–10) with 300 nM of each of the four Cas9–sgRNAs shown for 15 min at 37 °C. Expected cleavage products are 774–778 bp and 217–221 bp. M, 100-bp ladder; the lower two heavy bands are 500 and 1,000 bp. **b**, Quantification of DNA cleavage in **a** by densitometry using imageJ. **c**, Comparison of transfection efficiency in HEK293T cells and wild-type primary fibroblasts. Fifty nanograms GFP plasmid, 10 nM Cas9–FitC–Tmc1-mut3 sgRNA RNP, or 10 nM Cas9–CrRNA–Tmc1-mut3–atto-550-TracrRNA RNP were delivered into HEK293T cells or wild-type primary fibroblasts using 3 μl Lipofectamine 2000. For samples with GFP plasmid, the fraction of GFP-positive cells was measured by flow cytometry 24 h after delivery. For samples with Cas9–FitC–Tmc1-mut3 RNP or Cas9–CrRNA–Tmc1-mut3–atto-550-TracrRNA RNP, medium was removed 6 h after delivery. The cells were trypsinized, washed three times with 500 μl PBS containing 20 U ml^{-1} heparin, and subjected to flow cytometry. **d**, Wild-type or *Bth* mutant *Tmc1* allele editing in primary fibroblasts derived from wild-type or $Tmc1^{Bth/Bth}$ mice as a function of the dose of Cas9–Tmc1-mut3–lipid complex. Cas9–Tmc1-mut3 (12.5, 25, 50, 100, 200, or 400 nM) was delivered into the primary fibroblasts using Lipofectamine 2000 in DMEM–FBS. **e**, Lipid-mediated delivery of Cas9–sgRNA complexes into primary fibroblasts derived from wild-type or $Tmc1^{Bth/Bth}$ mice. We delivered 100 nM of purified Cas9 protein and each wild-type *Tmc1*-targeting sgRNA (Tmc1-wt1, Tmc1-wt2, or Tmc1-wt3) or $Tmc1^{Bth}$ mutant-targeting sgRNA (Tmc1-mut1, Tmc1-mut2, or Tmc1-mut3) into wild-type fibroblasts (red) and $Tmc1^{Bth/Bth}$ fibroblasts (blue) using Lipofectamine 2000 in DMEM–FBS. Primary fibroblast cells were harvested 96 h after treatment. Genomic DNA was extracted and indels were detected by HTS. Individual values ($n = 3$–4) are shown; horizontal lines and error bars represent mean ± s.d. of biological replicates.

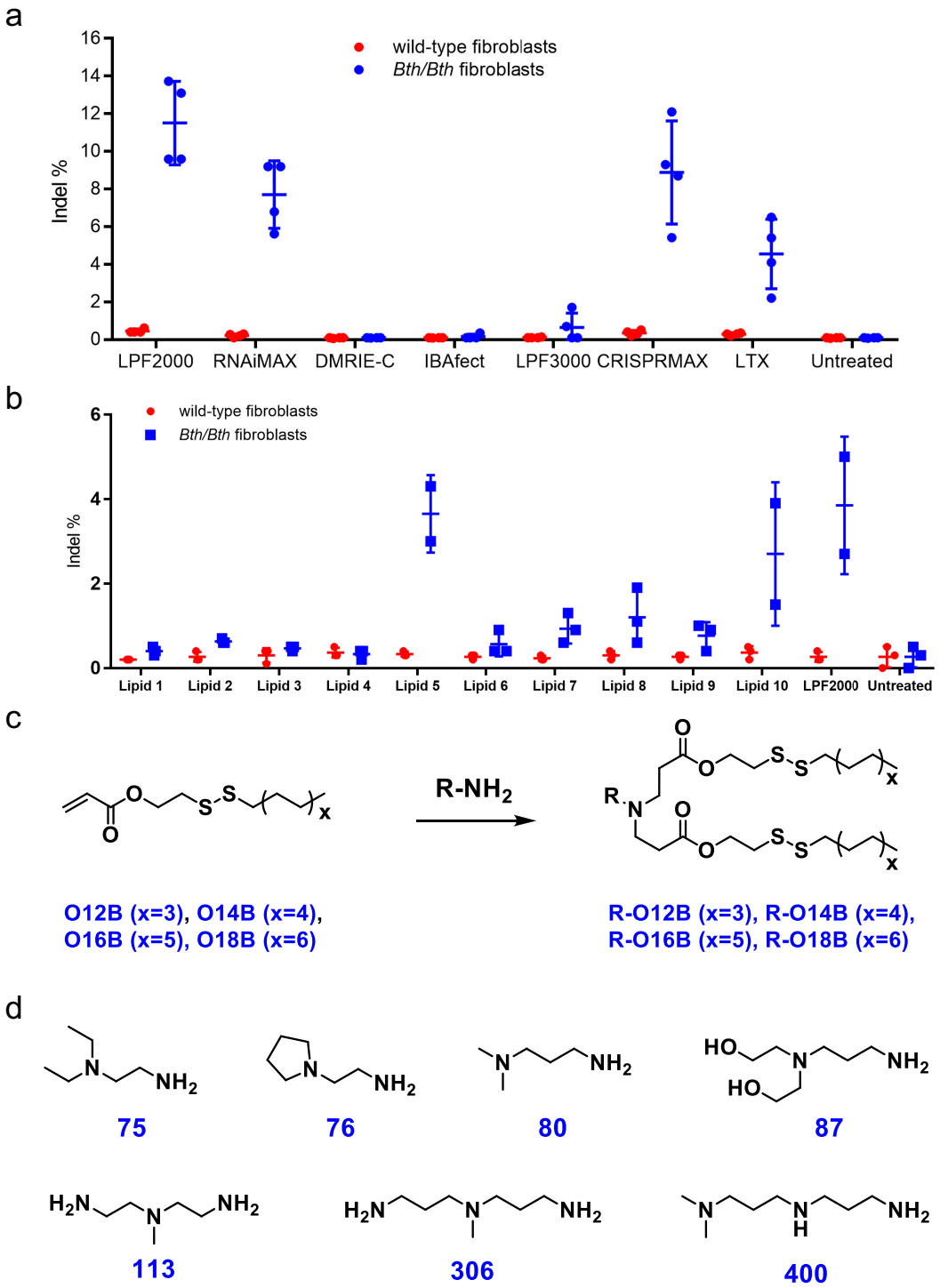

Extended Data Figure 2 | Delivery of Cas9–Tmc1-mut3 sgRNA complexes into primary fibroblasts derived from wild-type or homozygous *Tmc1*$^{Bth/Bth}$ mice. a, Using seven commercially available lipids: LPF2000 (Lipofectamine 2000); RNAiMAX (Lipofectamine RNAiMAX); LPF3000 (Lipofectamine 3000); CRISPRMAX (Lipofectamine CRISPRMAX); LTX (Lipofectamine LTX). **b**, Using ten biodegradable, bioreducible lipids: Lipid 1 (75-O14B); Lipid 2 (76-O14B); Lipid 3 (80-O18B); Lipid 4 (87-O16B); Lipid 5 (113-O18B); Lipid 6 (306-O12B); Lipid 7 (306-O16B); Lipid 8 (306-O18B); Lipid 9 (400-O12B); Lipid 10 (400-O16B). We delivered 100 nM purified Cas9–Tmc1-mut3 RNP using 3 μl of the cationic lipid shown in DMEM-FBS. Fibroblast cells were collected 96 h after treatment, genomic DNA was extracted, and indels were detected by HTS. **c**, Synthetic route and chemical structure of lipids. **d**, Commercially available amine head groups used in lipid synthesis. Lipids were synthesized as previously described[26]. Individual values ($n = 2$–4) are shown; horizontal lines and error bars represent mean ± s.d. of three or more biological replicates.

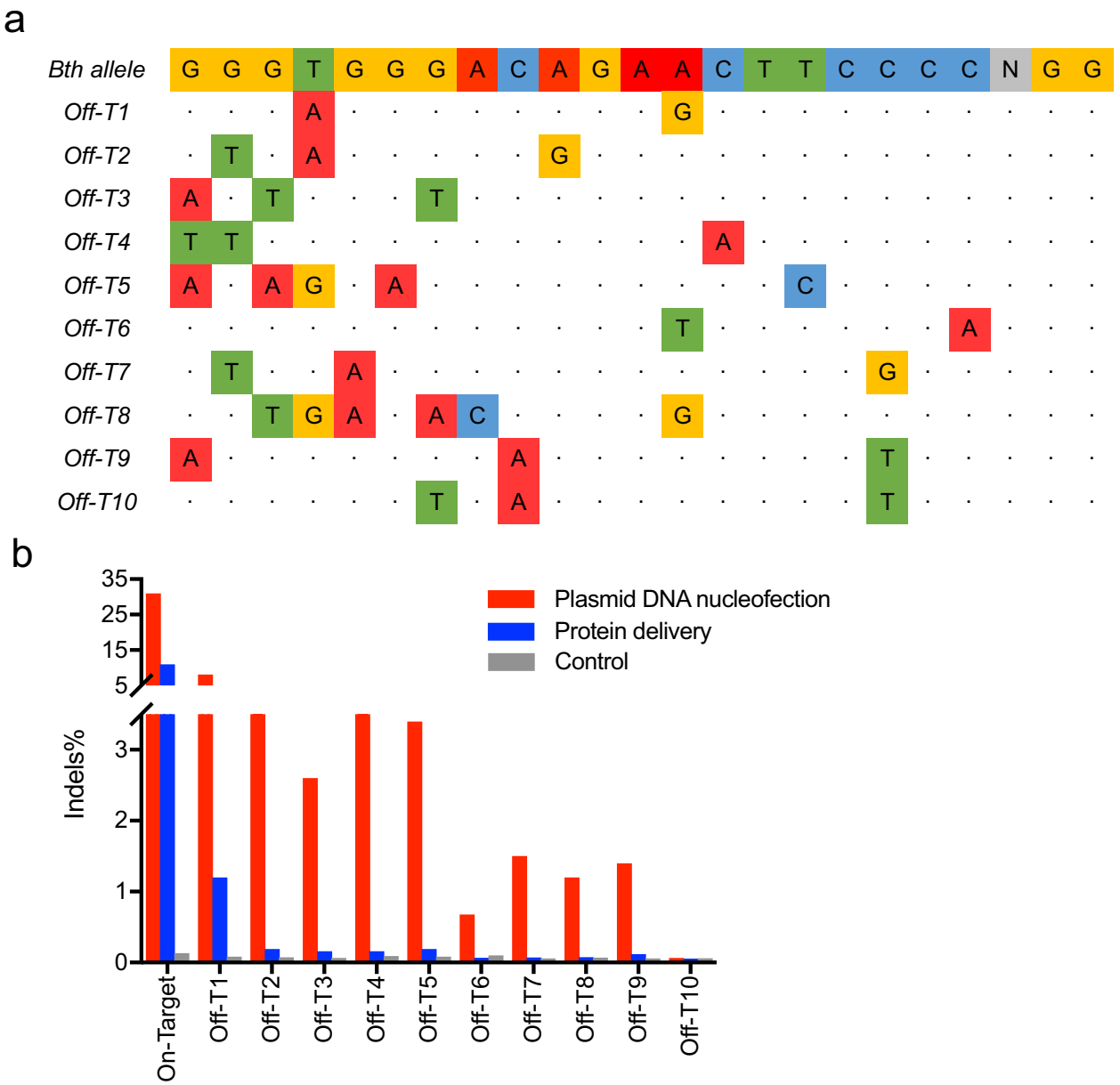

Extended Data Figure 3 | Off-target sites identified by GUIDE-seq after nucleofection of DNA plasmids encoding Cas9 and Tmc1-mut3 sgRNA into primary fibroblasts from *Tmc1*$^{Bth/+}$ mice. a, One thousand nanograms of Cas9 plasmid, 300 ng Tmc1-mut3 sgRNA plasmid, 400 ng pmaxGFP plasmid, and 50 pmol double-stranded oligodeoxynucleotides (dsODN) were nucleofected into *Tmc1*$^{Bth/+}$ fibroblasts using a LONZA 4D-Nucleofector. Genomic DNA was extracted 96 h after nucleofection and subjected to GUIDE-seq as previously described[23]. *Off-T1* to *Off-T10* are ten off-target sites detected by GUIDE-seq. Mismatches compared to the on-target site are shown and highlighted in colour. The *Tmc1*^{Bth} allele targeted by sgRNA Tmc1-mut3 is shown in the top row. **b**, Indel frequency at the *Tmc1* locus and at each of the off-target loci in Cas9–Tmc1-mut3-treated *Tmc1*$^{Bth/Bth}$ primary fibroblasts following plasmid DNA nucleofection or following RNP delivery. For RNP delivery, 100 nM Cas9–Tmc1-mut3 RNP was delivered to the *Tmc1*$^{Bth/Bth}$ fibroblasts using 3 μl Lipofectamine 2000. Indels were detected by HTS at the *Tmc1* on-target site and at each off-target site. Red, samples nucleofected with DNA plasmids encoding Cas9 and Tmc1-mut3 sgRNA; blue, samples treated with Cas9–Tmc1-mut3 RNPs; grey, control samples nucleofected with unrelated dsDNA only.

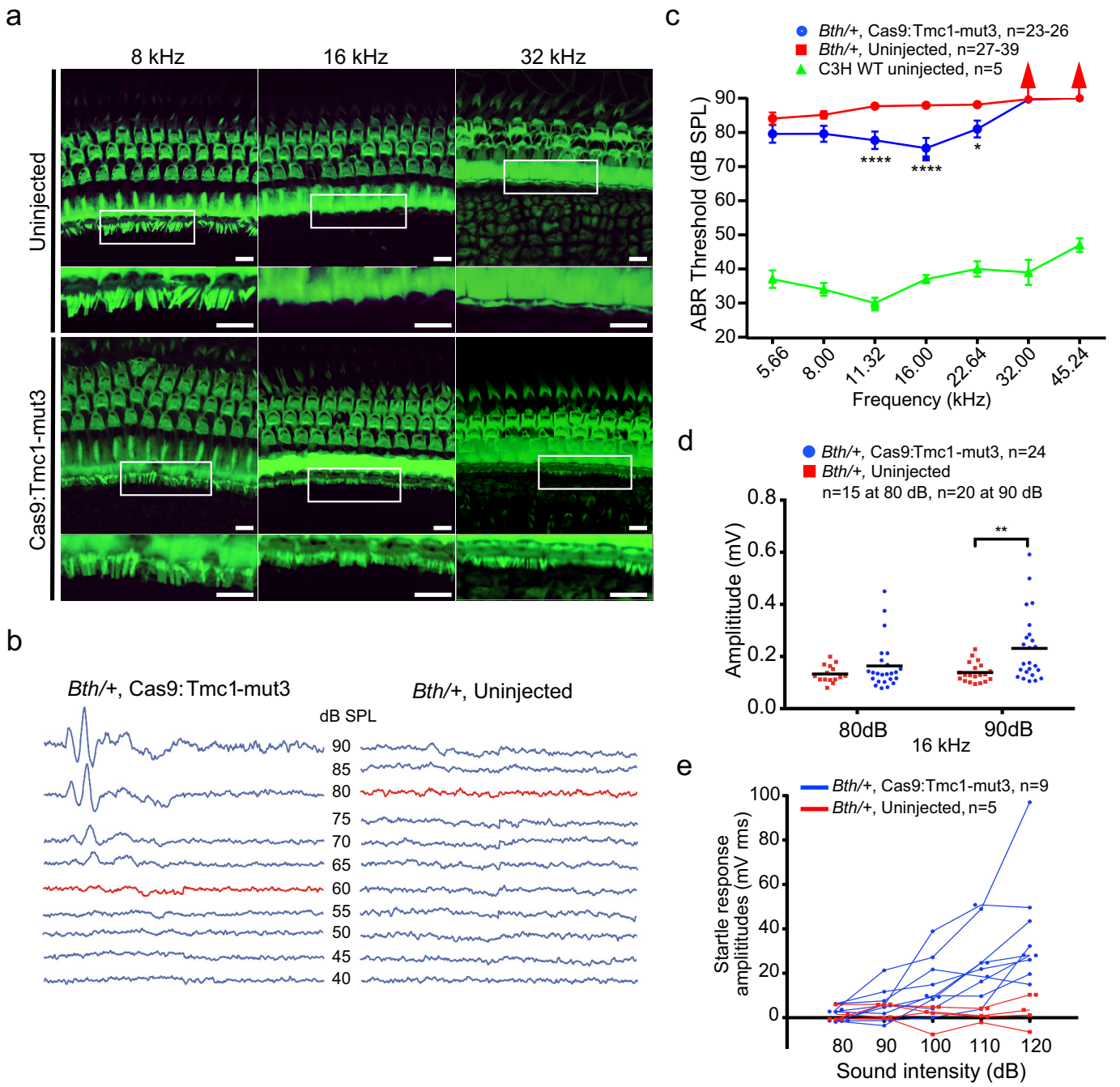

Extended Data Figure 4 | Cas9–Tmc1-mut3–lipid injection reduces hearing loss, improves acoustic startle response, and preserves stereocilia in *Tmc1*$^{Bth/+}$ mice. a, Phalloidin labelling showed the preservation of stereocilia of IHCs in an ear eight weeks after injection with Cas9–Tmc1-mut3 sgRNA at three frequency locations indicated, whereas the uninjected contralateral inner ear of the same mouse showed severe degeneration of stereocilia at locations corresponding to 16 and 32 kHz. The boxes indicate the stereocilia, which are shown at the bottom of each image at higher magnification. Scale bars, 10 μm. Similar results were observed in other injected ears that were immunolabelled ($n = 5$). **b**, Representative ABR waveforms showing reduced threshold (red traces) at 16 kHz in a Cas9–Tmc1-mut3–lipid-injected *Tmc1*$^{Bth/+}$ ear (left) compared to the uninjected contralateral ear (right) of the same mouse after four weeks. **c**, Eight weeks after Cas9–Tmc1-mut3 injection into *Tmc1*$^{Bth/+}$ ears (blue), mean ABR thresholds were significantly reduced at three frequencies. Uninjected *Tmc1*$^{Bth/+}$ ears (red) showed ABR thresholds >85 dB at all frequencies after eight weeks. ABR thresholds from wild-type C3H mice are shown in green. **d**, ABR wave 1 amplitudes following 90 dB SPL stimulation at 16 kHz were greater in injected *Tmc1*$^{Bth/+}$ ears than in uninjected ears eight weeks after treatment. Individual values ($n = 15$ or 20 for uninjected, and 24 for injected) are shown; horizontal bars represent mean values. **e**, Startle responses at 16 kHz in individual Cas9–Tmc1-mut3 sgRNA-injected mice (blue) were significantly stronger ($P < 0.001$) than in uninjected mice (red) eight weeks after treatment. Among the different frequencies assayed, the number of ears tested (n) varies within the range shown (Supplementary Table 2). Statistical analyses of ABR thresholds, amplitudes, and startle responses were performed by two-way ANOVA with Bonferroni correction for multiple comparisons: *$P < 0.05$, **$P < 0.01$, ****$P < 0.0001$. Values and error bars reflect mean ± s.e.m.

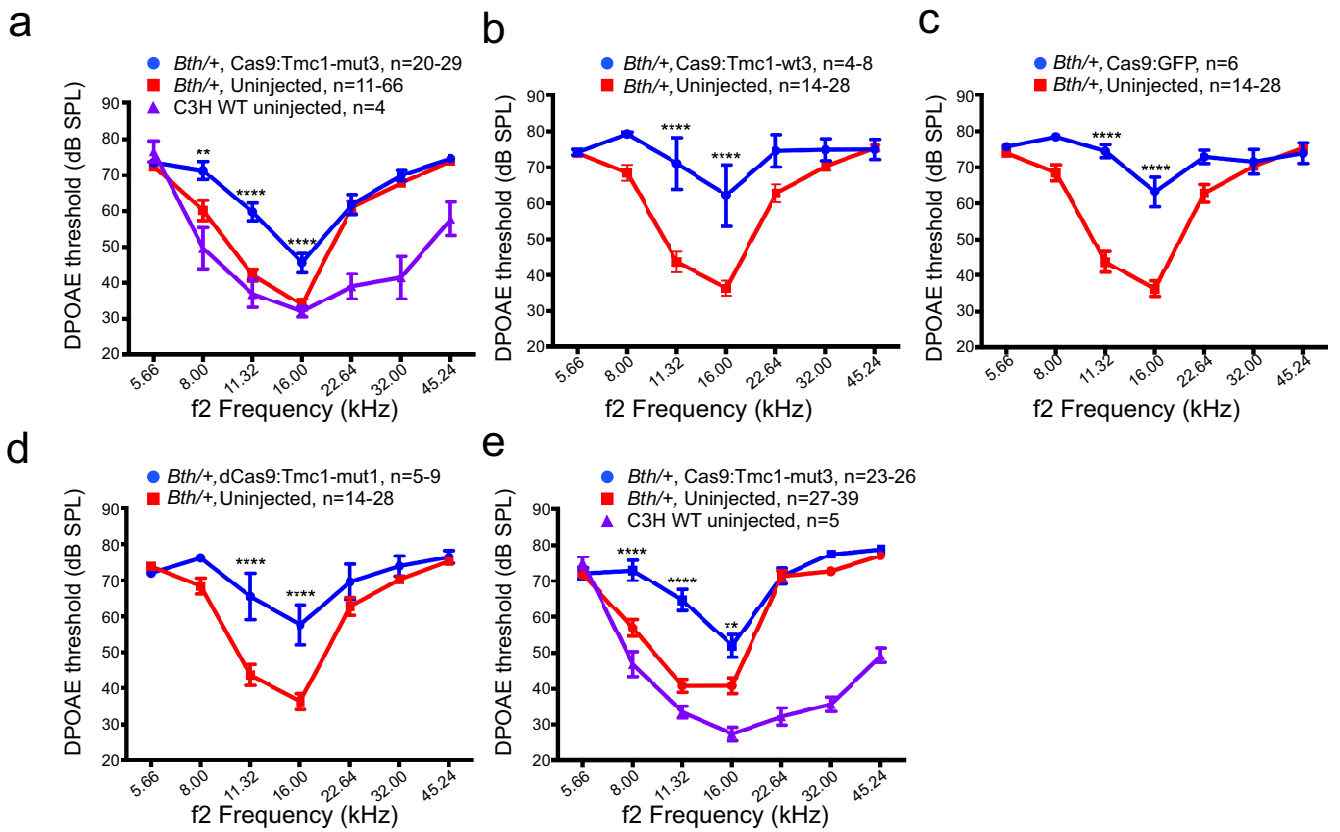

Extended Data Figure 5 | Effect of *in vivo* injection of Cas9–sgRNA–lipid complexes on DPOAE thresholds. a–d, DPOAE thresholds four weeks after injection were elevated compared with uninjected ears at three frequencies following treatment with Cas9–Tmc1-mut3 sgRNA (**a**), and were elevated at two frequencies following treatment with Cas9–Tmc1-wt3 sgRNA (**b**), Cas9–GFP sgRNA (**c**), or dCas9–Tmc1-mut1 sgRNA (**d**). **e**, Eight weeks after Cas9–Tmc1-mut3 sgRNA injection, DPOAE thresholds were elevated at three frequencies in the injected group. Mean DPOAE thresholds of untreated wild-type (WT) C3H mice at four weeks (**a**) or eight weeks (**e**) of age are also shown in purple. Statistical analysis of DPOAE thresholds was performed by two-way ANOVA with Bonferroni correction for multiple comparisons: $^{**}P < 0.01$, $^{****}P < 0.0001$. Values and error bars reflect mean ± s.e.m. Among the different frequencies assayed, the number of ears tested (n) varies within the range shown (Supplementary Table 2). The elevation of DPOAE thresholds despite enhanced hair cell survival (Fig. 2d, g) suggests that the surviving OHCs may not be fully functional. IHCs can respond to sound and excite auditory nerve fibres in the absence of OHC amplification, although at higher SPLs. Thus, an improvement in ABR thresholds and suprathreshold amplitudes can occur without concomitant DPOAE enhancement if the functional improvements are restricted to the surviving IHCs.

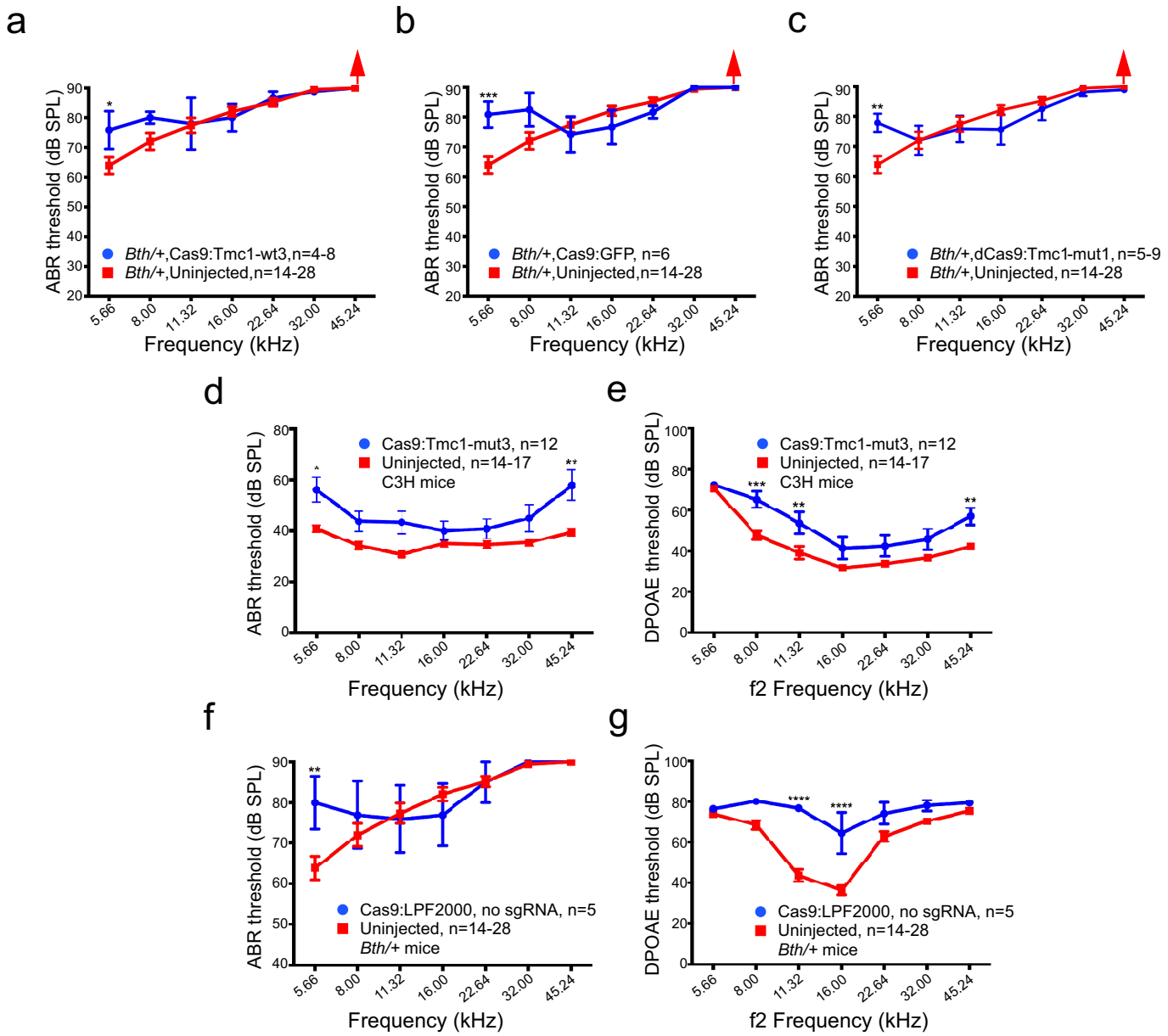

Extended Data Figure 6 | Hearing rescue is dependent on the *Tmc1*^{Bth} target specificity of the sgRNA, Cas9 nuclease activity, the presence of the *Tmc1*^{Bth} mutation, and the presence of the sgRNA. a, In *Tmc1*$^{Bth/+}$ ears injected with Cas9–Tmc1-wt3–lipid, which targets the wild-type *Tmc1* allele instead of the mutant *Tmc1*^{Bth} allele, ABR thresholds (blue) were comparable to or higher than those of uninjected controls (red) after four weeks. **b**, *Tmc1*$^{Bth/+}$ ears injected with Cas9–GFP sgRNA–lipid (blue) did not show improved ABR thresholds four weeks after treatment. **c**, *Tmc1*$^{Bth/+}$ ears injected with catalytically inactive dCas9–Tmc1-mut1–lipid did not show improved ABR thresholds four weeks after treatment. **d**, ABR thresholds of wild-type C3H mice injected with Cas9–Tmc1-mut3–lipid showed similar patterns to the uninjected control inner ears at four weeks, except at 5.66 and 45.24 kHz where ABR thresholds were elevated. **e**, Elevated DPOAE thresholds at three frequencies were observed after the treatment in **d**. **f**, Injection of Cas9–Lipofectamine 2000 (LPF2000) without sgRNA in *Tmc1*$^{Bth/+}$ mice did not improve ABR thresholds after four weeks. **g**, Elevated DPOAE thresholds at 11 and 16 kHz were observed after the treatment in **f**. Statistical analysis of ABR and DPOAE thresholds was performed by two-way ANOVA with Bonferroni correction for multiple comparisons: $^{*}P < 0.05$, $^{**}P < 0.01$, $^{***}P < 0.001$, $^{****}P < 0.0001$. Values and error bars reflect mean ± s.e.m. Among the different frequencies assayed, the number of ears tested (n) varies within the range shown (Supplementary Table 2).

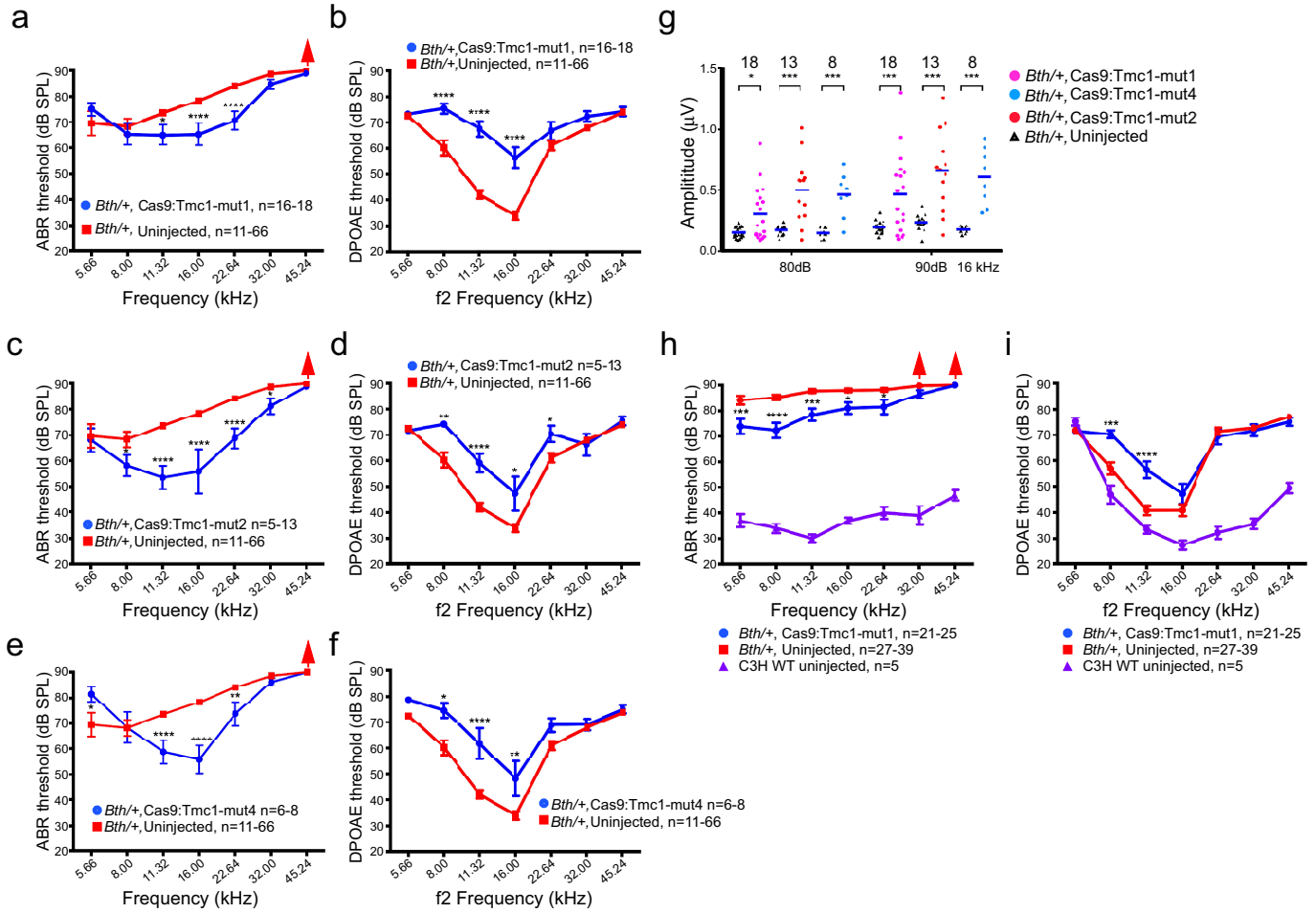

Extended Data Figure 7 | Hearing preservation following treatment with additional Tmc1-mut sgRNAs other than Tmc1-mut3. a, Mean ABR thresholds were significantly reduced at three frequencies in ears injected with Cas9–Tmc1-mut1–lipid compared to uninjected $Tmc1^{Bth/+}$ ears after four weeks. **b**, DPOAE thresholds were elevated in the same group of inner ears after Cas9–Tmc1-mut1 injection as in **a** after four weeks. **c**, Mean ABR thresholds were significantly reduced at five frequencies in ears injected with Cas9–Tmc1-mut2–lipid compared to uninjected $Tmc1^{Bth/+}$ ears after four weeks. **d**, DPOAE thresholds were elevated in the same group of inner ears after Cas9–Tmc1-mut2 injection as in **c** after four weeks. **e**, Mean ABR thresholds were significantly reduced at three frequencies in ears injected with Cas9–Tmc1-mut4–lipid compared to uninjected $Tmc1^{Bth/+}$ ears after four weeks. **f**, DPOAE thresholds were elevated in the same group of inner ears after Cas9–Tmc1-mut4–lipid injection as in **e** after four weeks. **g**, Significantly stronger wave 1 amplitudes were detected in ears injected with each of the Cas9–Tmc1-mut–lipid complexes shown at 16 kHz (80 and 90 dB SPL). Individual values ($n = 8$, 13, or 18) are shown; horizontal bars represent mean values. **h**, Eight weeks after Cas9–Tmc1-mut1–lipid injection into $Tmc1^{Bth/+}$ ears, mean ABR thresholds were significantly reduced at five frequencies compared to uninjected $Tmc1^{Bth/+}$ ears, which showed ABR thresholds >80 dB at all frequencies after eight weeks. Mean ABR thresholds of untreated wild-type (WT) C3H mice of eight weeks of age are shown in purple. Red arrows indicate no ABR response at the highest SPL level of 90 dB. **i**, DPOAE thresholds were significantly elevated at two frequencies (8 and 11 kHz) in the same group of inner ears after Cas9–Tmc1-mut1 injection as in **h** after eight weeks. Mean DPOAE thresholds of untreated wild-type C3H mice of eight weeks of age are shown in purple. Statistical analysis of ABR and DPOAE thresholds and wave 1 amplitudes was performed by two-way ANOVA with Bonferroni correction for multiple comparisons: $^*P < 0.05$, $^{**}P < 0.01$, $^{***}P < 0.001$, $^{****}P < 0.0001$. Values and error bars reflect mean ± s.e.m. Among the different frequencies assayed, the number of ears tested (n) varies within the range shown (Supplementary Table 2).

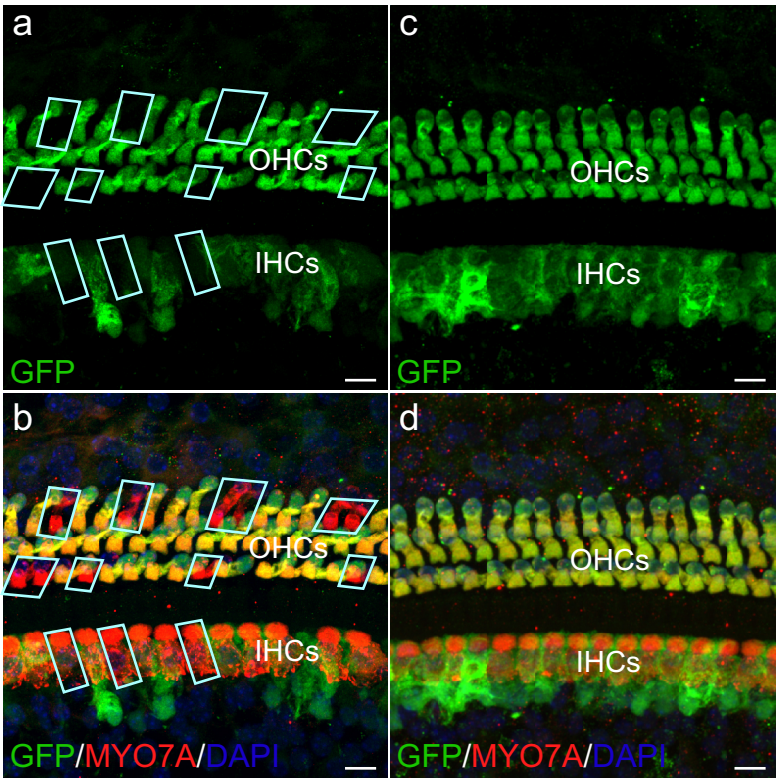

Extended Data Figure 8 | RNP delivery of Cas9–sgRNA–lipid complexes results in genome editing in adult hair cells. Six-week-old adult Atoh1–GFP cochlea were injected with 1 μl 25 μM Cas9–GFP sgRNA–lipid complex by canalostomy, with the cochlea removed two weeks after injection. **a**, Genome editing was detected by the loss of GFP (green, with GFP absence noted using cyan shapes) in inner hair cells (IHCs) and outer hair cells (OHCs). **b**, Hair cells were labelled with the hair cell marker MYO7A (red) in the apex turn of cochlea. **c**, **d**, In uninjected contralateral Atoh1–GFP cochlea, all hair cells were GFP-positive. Scale bars, 10 μm. Similar results were observed in other injected ears that were immunolabelled ($n = 3$).

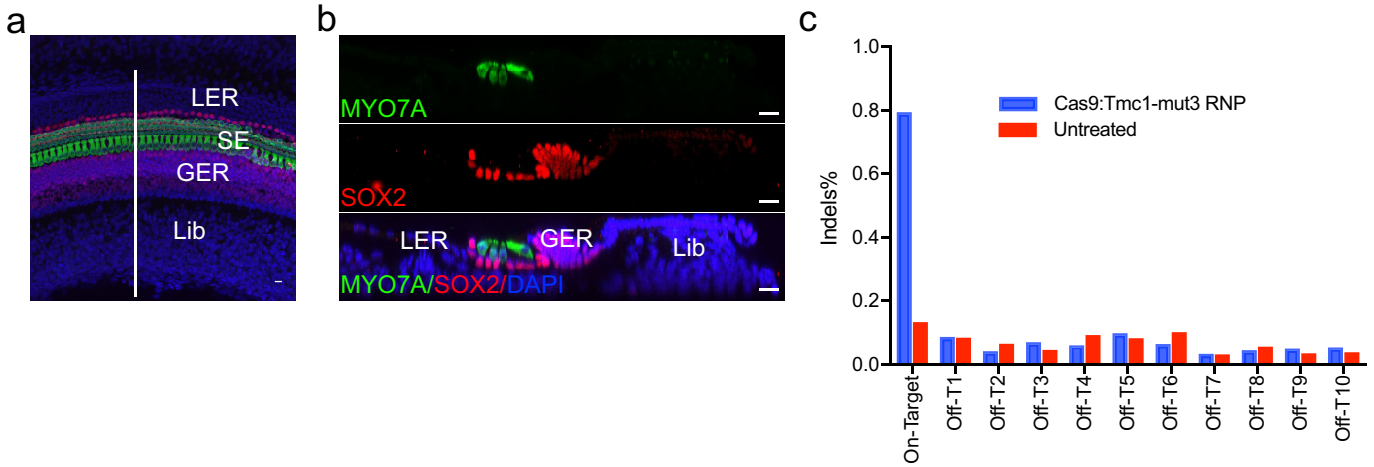

Extended Data Figure 9 | *In vivo* editing of the *Tmc1* locus from *Tmc1*$^{Bth/+}$ ears injected with Cas9–Tmc1-mut3 sgRNA. A representation of the organ of Corti removed at P5 for high-throughput DNA sequencing. **a**, A confocal *z*-stack image showing the surface view of a dissected and labelled organ of Corti used for HTS. **b**, A cross-sectional view of the organ of Corti (along the white line in **a**) showing the positions of hair cells (MYO7A), supporting cells (SOX2) and the cells from other cochlear regions that were used for quantification. LER, lesser epithelial ridge; GER, greater epithelial ridge; SE, sensory epithelium; Lib, limbus region. DAPI-labelled nuclei are shown in blue. Quantification showed that hair cells represented 1.45% ± 0.05% (mean ± s.e.m., $n = 4$) of all cells in the dissected cochlea. Scale bars, 10 μm. **c**, On-target and off-target *in vivo* editing of the *Tmc1* locus in organ of Corti samples. No indels were observed at frequencies substantially above that of an untreated control sample at any of the ten off-target sites identified by GUIDE-seq (*Off-T1* to *Off-T10*). Indels were detected by HTS at the *Tmc1* on-target site and each off-target site from *in vivo* tissue samples dissected from the inner ear of neonatal mice 4 days after Cas9–Tmc1-mut3 RNP injection (blue), or from untreated control samples (red).

Extended Data Table 1 | Off-target editing after nucleofection of DNA plasmids encoding Cas9 and Tmc1-mut3 sgRNA into primary fibroblasts derived from *Tmc1*$^{Bth/Bth}$ mice

a

	5'-Sequence-3'	Mismatches (MMs)	NCBI accession	Predicted function	Location	Indels in *Bth/Bth*
Bth	GGGTGGGACAGAACTTCCCCAGG	0MMs	N/A		chr9	31%
Off-T1	GGGAGGGACAGAGCTTCCCCAGG	2MMs [4:13]	N/A		chr1	8.1%
Off-T2	GTGAGGGAGAGAACTTCCCCTGG	3MMs [2:4:9]	N/A		chr16	4.4%
Off-T3	AGTTGGTACAGAACTTCCCCAGG	3MMs [1:3:7]	NC_000068.7	CD82 antigen	chr2	2.6%
Off-T4	TTGTGGGACAGAAATTCCCCAGG	3MMs [1:2:14]	N/A		chr12	3.9%
Off-T5	AGAGGAGACAGAACTCCCCCAGG	5MMs [1:3:4:6:16]	N/A		chr13	3.4%
Off-T6	GGGTGGGACAGATCTTCCCAGGG	2MMs [13:20]	NC_000067.6	hemicentin-1 isoform	chr1	0.68%
Off-T7	GTGTAGGACAGAACTTCGCCAGG	3MMs [2:5:18]	XM_006507026.3	inositol 1,4,5-triphosphate receptor 2	chr6	1.5%
Off-T8	GGTGAGACCAGAGCTTCCCCTGG	6MMs [3:4:5:7:8:13]	XR_389309.3	unknown	chr5	1.2%
Off-T9	AGGTGGGAAAGAACTTCTCCGGG	3MMs [1:9:18]	NC_000070.6	paralemmin A kinase anchor protein	chr4	1.4%
Off-T10	GGGTGGTAAAGAACTTCTCCTGG	3MMs [7:9:18]	N/A		chr10	0.048%

b

	5'-Sequence-3'	Mismatches	NCBI accession	Location	Indels in *Bth/Bth*
Bth	GGGTGGGACAGAACTTCCCCAGG	0MMs		chr9	31%
Off-T1'	GGGAGGGACAGAGCTTCCCCAGG	2MMs [4:13]		chr1	8.1%
Off-T2'	GTGAGGGAGAGAACTTCCCCTGG	3MMs [2:4:9]		chr16	4.4%
Off-T3'	AGGAAGGCCAGAACTTCCCCTAG	4MMs [1:4:5:8]	NM_001312644.1	chr12	0.037%
Off-T4'	GGAGGGGGCTGAACTTCCCCAGG	4MMs [3:4:8:10]		chr9	0.071%
Off-T5'	GTGTGGAACAGAACTTCCCAGGG	3MMs [2:7:20]		chr1	0.046%
Off-T6'	CCCTGGAACAGAACTTCCCCAAG	4MMs [1:2:3:7]		chr2	0.097%
Off-T7'	GCGCGGGACAGAACATCCCCTAG	3MMs [2:4:15]		chr5	0.033%
Off-T8'	AGGCAGGACAAAACTTCCCCAAG	4MMs [1:4:5:11]		chr1	0.091%

a, Off-target sites identified by GUIDE-seq[23]. Mismatch positions are indicated, counting the PAM as positions 21–23. *Off-T3, Off-T6, Off-T7, Off-T8* and *Off-T9* are located within predicted gene regions, while the rest are intergenic. One thousand nanograms Cas9 plasmid and 300 ng Tmc1-mut3 sgRNA plasmid were nucleofected into *Tmc1*$^{Bth/Bth}$ fibroblasts using a LONZA 4D-Nucleofector and indels were detected by HTS at Tm *Tmc1*^{Bth} on-target and each off-target site. Mismatches compared to the on-target sequence are shown in red and PAMs are in blue. **b**, Off-target sites identified by computational prediction using the CRISPR Design Tool[24]. Among the top eight computationally predicted off-target sites, only two (*off-T1'* and *off-T2'* with two and three mismatches, respectively) were identified as bona fide off-targets in cells by GUIDE-seq.

nature research

Corresponding author(s): David R. Liu and Zheng-Yi Chen

☐ Initial submission ☐ Revised version ☒ Final submission

Life Sciences Reporting Summary

Nature Research wishes to improve the reproducibility of the work that we publish. This form is intended for publication with all accepted life science papers and provides structure for consistency and transparency in reporting. Every life science submission will use this form; some list items might not apply to an individual manuscript, but all fields must be completed for clarity.

For further information on the points included in this form, see Reporting Life Sciences Research. For further information on Nature Research policies, including our data availability policy, see Authors & Referees and the Editorial Policy Checklist.

Experimental design

1. Sample size

Describe how sample size was determined.

For hair cell transduction current recording, a minimum of 6 hair cells (6-18) were recorded for each condition. In experimental groups to show reproducible and robust hearing, we used a minimum of 11 animals (from 11 to 30) for each of the frequency studied. For auditory startle evaluation, we used 9 injected animals to better measure the response and variations, and used 5 uninjected control animals due to their uniform unresponsiveness. We used a minimum of 4 animals in all control studies. Other experiments were done in biological triplicate, n=3 on different days. In previous studies we determined this sample size to be sufficient to ensure reproducibility.

2. Data exclusions

Describe any data exclusions.

For ABR measurements, a small fraction of frequencies for which thresholds were not apparent were excluded to ensure that only ABR thresholds scored accurately were used.

3. Replication

Describe whether the experimental findings were reliably reproduced.

All the experimental findings were replicated with the number of replicates, animals and variations shown by n, SD (in vitro assays), and SEM (in vivo experiments).

4. Randomization

Describe how samples/organisms/participants were allocated into experimental groups.

The animals of the same genotypes (Bth/+ or C3H) were randomly chosen to be in experimental or control groups according to experimental design.

5. Blinding

Describe whether the investigators were blinded to group allocation during data collection and/or analysis.

All data from in vivo experiments were collected and analyzed by at least two researchers who were both blinded to experiment.

Note: all studies involving animals and/or human research participants must disclose whether blinding and randomization were used.

6. Statistical parameters

For all figures and tables that use statistical methods, confirm that the following items are present in relevant figure legends (or in the Methods section if additional space is needed).

n/a	Confirmed
☐	☒ The exact sample size (*n*) for each experimental group/condition, given as a discrete number and unit of measurement (animals, litters, cultures, etc.)
☐	☒ A description of how samples were collected, noting whether measurements were taken from distinct samples or whether the same sample was measured repeatedly
☐	☒ A statement indicating how many times each experiment was replicated
☐	☒ The statistical test(s) used and whether they are one- or two-sided (note: only common tests should be described solely by name; more complex techniques should be described in the Methods section)
☐	☒ A description of any assumptions or corrections, such as an adjustment for multiple comparisons
☐	☒ The test results (e.g. *P* values) given as exact values whenever possible and with confidence intervals noted
☐	☒ A clear description of statistics including central tendency (e.g. median, mean) and variation (e.g. standard deviation, interquartile range)
☐	☒ Clearly defined error bars

See the web collection on statistics for biologists for further resources and guidance.

Software

Policy information about availability of computer code

7. Software

Describe the software used to analyze the data in this study.

Prism 6 from GraphPad was used for statistic analysis. Matlab were used for indel-identification and acoustic startle reflex data analyses. ImageJ (NIH image) was used for IHC and OHC counting. Adobe Photoshop CS3 was used to composite images showing the whole cochlea. Custom LabVIEW software controlling National Instruments 24-bit soundcards (6052E) generated all ABR/DPOAE stimuli and recorded all responses.

For manuscripts utilizing custom algorithms or software that are central to the paper but not yet described in the published literature, software must be made available to editors and reviewers upon request. We strongly encourage code deposition in a community repository (e.g. GitHub). *Nature Methods* guidance for providing algorithms and software for publication provides further information on this topic.

Materials and reagents

Policy information about availability of materials

8. Materials availability

Indicate whether there are restrictions on availability of unique materials or if these materials are only available for distribution by a for-profit company.

No unique materials were used.

9. Antibodies

Describe the antibodies used and how they were validated for use in the system under study (i.e. assay and species).

Immunofluorescence: rabbit anti-MYO7A (25-6790, Proteus BioSciences), chicken anti-GFP (ab13970, Abcam), goat anti-SOX2 (sc-17320, Santa Cruz Biotechnology), goat anti-chicken Alexa Fluor 488 (A-11039, Invitrogen), donkey anti-rabbit Alex488 (A21206) or Alex 594 (A21207), donkey anti goat Alex594 (A11058), and Alexa-488-phalloidin (A12379). All of them have been used in previously published studies on the adult mouse cochlea (Shu et al.,Hum Gene Ther. 2016 Sep;27(9):687-99; Huang et al., J Neurosci. 2013 Sep 18;33(38):15086-94; Kurima et al., 2015, Cell Reports 12, 1606–1617)

10. Eukaryotic cell lines

a. State the source of each eukaryotic cell line used.

HEK293T cells were originally purchased from ATCC (catlog CRL-3216).
Wild-type, Bth/+ and Bth/Bth fibroblasts were obtained from P5 pups.

b. Describe the method of cell line authentication used.

HEK293T (catlog CRL-3216) is a commercial cell line and authenticated by ATCC.
Primary fibroblasts from Bth mice were genotyped by the lab.

c. Report whether the cell lines were tested for mycoplasma contamination.

All cell lines tested negative for mycoplasma contamination.

d. If any of the cell lines used are listed in the database of commonly misidentified cell lines maintained by ICLAC, provide a scientific rationale for their use.

No commonly misidentified cell lines were used.

Animals and human research participants

Policy information about studies involving animals; when reporting animal research, follow the ARRIVE guidelines

11. Description of research animals

Provide details on animals and/or animal-derived materials used in the study.

Mouse strains used in this study are:
C3HeB/FeJ (C3H),
heterozygous Tmc1 Bth/+ , in C3H background
homozygous Bth/Bth, in C3H background
Tmc1 Bth/Bth;Tmc2 Δ/Δ, in C3H background
Tmc1 Δ/Δ;Tmc2 Δ/Δ, in C3H background
Mice of either sex at P0-P6 were used for culture and injection. Acoustic tests were performed 1-2 month after the injection.

Policy information about studies involving human research participants

12. Description of human research participants

Describe the covariate-relevant population characteristics of the human research participants.

The research did not involve human research participants.

nature research

Corresponding author(s): David R. Liu and Zheng-Yi Chen

☐ Initial submission ☐ Revised version ☒ Final submission

Flow Cytometry Reporting Summary

Form fields will expand as needed. Please do not leave fields blank.

Data presentation

For all flow cytometry data, confirm that:

☒ 1. The axis labels state the marker and fluorochrome used (e.g. CD4-FITC).

☒ 2. The axis scales are clearly visible. Include numbers along axes only for bottom left plot of group (a 'group' is an analysis of identical markers).

☒ 3. All plots are contour plots with outliers or pseudocolor plots.

☒ 4. A numerical value for number of cells or percentage (with statistics) is provided.

Methodological details

5. Describe the sample preparation.	For samples with GFP plasmid transfection, the fraction of cells with GFP expression was measured by flow cytometry 24 h after delivery. For samples treated with Cas9: FitC-Tmc1-mut3 RNP, or Cas9:CrRNA-Tmc1-mut3:atto-550-TracrRNA RNP, media was removed 6 h after delivery. The cells were trypsinized, washed three times with 500 µL PBS containing 20 U/mL heparin, and prepared for counting and flow cytometry.
6. Identify the instrument used for data collection.	Beckman Coulter Cytoflex
7. Describe the software used to collect and analyze the flow cytometry data.	CytExpert
8. Describe the abundance of the relevant cell populations within post-sort fractions.	The purity of cells was high as determined by microscopy.
9. Describe the gating strategy used.	Cells lacking the treatment of interest were used as negative controls for gating. For RNP delivery samples (FitC or Atto-550), control samples of fluorescent RNP only (without Lipofectamine 2000) were used for delivery to determine the efficiency of the washing procedure to remove extracellularly bound RNPs. The gating is the same with untreated samples.

Tick this box to confirm that a figure exemplifying the gating strategy is provided in the Supplementary Information. ☐